ZSoil

for geotechnics & structures

HOEK-BROWN MODEL FOR ROCKS

Report 140617

(revised 17.06.2014)

A. Truty

GeoDev.

PO Box CH-1001 Lausanne
Switzerland
https://zsoil.com

Contents

Chapter 1

Introduction

All derivations enclosed in this document are made using standard soil mechanics notation (all stresses are effective and positive in compression). In the following chapters complete theory for the standard Hoek-Brown model (2002 edition [2]) is given, then its extension to hardening/softening/stress and strain dependent dilatancy are disscussed [4]. All basic ingredients of the model are verified on certain set of benchmark problems. As the model may exhibit strain softening a special class of regularization (scaling softening modulus approach) is introduced to circumvent mesh dependencies. Details of the numerical implementation in ZSoil code [6] are not included in this report.

Chapter 2

Theory

2.1 Definition of the Hoek-Brown yield criterion

Window 2-1: Hoek-Brown criterion (2002 edition)

ZSoil®

The 2002 edition of Hoek-Brown criterion is described by the following equation

$$f(\sigma_1, \sigma_3) = \sigma_1 - \sigma_3 - \sigma_{ci} \left(m_b \frac{\sigma_3}{\sigma_{ci}} + s \right)^a$$

where σ_1 and σ_3 are the major and minor principal streses. The compressive strength of intact rock is denoted by σ_{ci} while the remaining three parameters a,s,m_b are usually related to the GSI index through the following expressions The compresive strength of intact rock is denoted by σ_{ci} while the remaining three parameters a,s,m_b are usually related to the GSI index through the following expressions

$$\begin{aligned} m_b &= m_i \, \exp\left(\frac{\mathsf{GSI} - 100}{28 - 14\, D} \right) \quad a = \frac{1}{2} + \frac{1}{6} \left(\exp\left(-\mathsf{GSI}/15 \right) - \exp\left(-20/3 \right) \right) \\ s &= \exp\left(\frac{\mathsf{GSI} - 100}{9 - 3\, D} \right) \end{aligned}$$

In the above expressions m_b is the reduced value of m_i parameter, while D is a factor that depends on degree of disturbance. D may vary from value 0.0 for undisturbed rock mass up to value 1.0 for highly disturbed one. The corresponding uniaxial compressive and biaxial tensile strengths can be derived from the yield criterion and expressed as follows

$$f_{tb}^{HB} = -\frac{s\, \sigma_{ci}}{m_b} \qquad f_c^{HB} = \sigma_{ci}\, s^a$$

The uniaxial tensile strength can be derived analytically only for $a = 0.5$ (for $a \neq 0.5$ iterative method has to be used)

$$f_t^{HB} = \frac{\sigma_{ci}}{2} \left(m_b - \sqrt{m_b^2 + 4s} \right)$$

Window 2-1

Window 2-2: Rankine criterion

ZSoil®

The Rankine (tensile cut-off) criterion is described as follows

$$f(\sigma_3) = -\sigma_3 + f_t = 0$$

where f_t is the uniaxial tensile strength. This f_t value must fulfill the condition $|f_t| < |f_t^{HB}|$ in order to preserve convexity of the resulting elastic domain. The main goal to introduce that criterion is such that it simplifies description of failure and dilatancy under tension.

Window 2-2

2.2 Running stability analysis with Hoek-Brown model

Window 2-3: Stability analysis using standard Hoek-Brown+Rankine criteria

ZSoil®

The only stability driver that can be used in conjunction with the Hoek-Brown model is the one based on stress level definition. In order to introduce safety factor to this criterion we can express it in the modified form

$$f(\sigma_1, \sigma_3) = \sigma_1 - \sigma_3 - \frac{1}{\mathsf{SF}}\sigma_{ci}\left(m_b \frac{\sigma_3}{\sigma_{ci}} + s\right)^a$$

$$f(\sigma_1, \sigma_3) = \sigma_1 - \sigma_3 - \left[\left(\mathsf{SF}^{-1}\right)^{\frac{1}{a}}\right]^a \sigma_{ci}\left(m_b \frac{\sigma_3}{\sigma_{ci}} + s\right)^a$$

Hence the final form of the yield criterion is expressed by means of the modified m_b^* and s^* parameters

$$f(\sigma_1, \sigma_3) = \sigma_1 - \sigma_3 - \sigma_{ci}\left(m_b^* \frac{\sigma_3}{\sigma_{ci}} + s^*\right)^a$$

$$\begin{aligned} m_b^* &= m_b \;\; \mathsf{SF}^{-\dfrac{1}{a}} \\ s^* &= s \;\; \mathsf{SF}^{-\dfrac{1}{a}} \end{aligned}$$

For the Rankine criterion standard reduction is used

$$f_t^* = \frac{f_t}{SF}$$

Window 2-3

2.3 Flow rules and dilatancy

Window 2-4: Contractant/dilatant flow rule for Hoek-Brown mechanism

ZSoil®

In the current implementation the plastic flow vector, expressed in the principal axes, is defined as follows

$$
\begin{aligned}
r_1^{HB} &= \quad (1 - \sin\psi\,(\sigma_3, \gamma^p)) \\
r_2^{HB} &= \quad 0 \\
r_3^{HB} &= -\,(1 + \sin\psi\,(\sigma_3, \gamma^p))
\end{aligned}
$$

In the basic setup one may assume that dilatancy angle ψ is a constant. However, triaxial compression tests indicate, that at a certain value of the confining stress $\sigma_3 = \sigma_\psi$, plastic volume changes become negligible. Such a stress dependent dilatancy law is shown in the figure below. For $\sigma_3 < 0$ (tensile stress) the dilatancy angle ψ is kept constant.

In the most advanced setup, both hardening and softening phenomena can be activated. In that case one may also relate value of the angle of dilatancy, at $\sigma_3 = 0$, to the current value of the deviatoric plastic strain γ^p.

The current angle of dilatancy $\overline{\psi}_o$ set up at $\sigma_3 = 0$ is expressed as follows

$$\overline{\psi}_o = \psi_o\, f_\psi^\gamma(\gamma^p)$$

where ψ_o can be understood as a fully mobilized dilatancy angle set up in the uniaxial compression test ($\sigma_3 = 0$).

The $f_\psi^\gamma(\gamma^p)$ is a piecewise linear function of plastic accumulated deviatoric strain γ_p. It is set up at $\gamma^p = 0$, $\gamma^p = \gamma_r$ and $\gamma_p = \gamma_{res}$. This way one may include an effect of initial contractancy ($f_\psi < 0$) during hardening (see second figure). It should be underlined here that dilatancy angle is both stress and strain dependent.

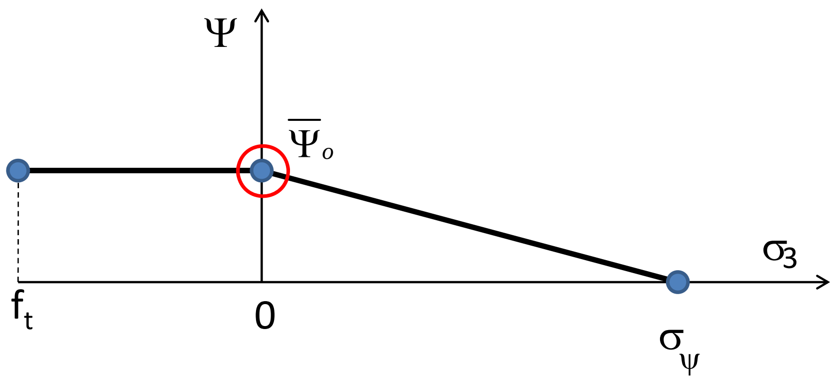

Relation between fully mobilized dilatancy angle and minor confining stress σ_3

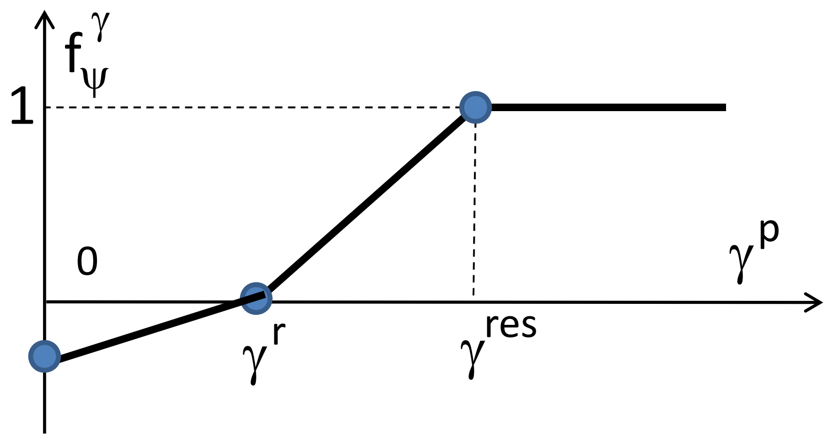

Evolution of $f_\psi^\gamma(\gamma^p)$ function

$$\psi = \begin{cases} \psi_o\, f_\psi^\gamma(\gamma_p) & \text{for} \quad \sigma_3 \leq 0 \\ \psi_o\, f_\psi^\gamma(\gamma_p)\left(1 - \dfrac{\sigma_3}{\sigma_\psi}\right) & \text{for} \quad 0 < \sigma_3 \leq \sigma_\psi \\ 0 & \text{for} \quad \sigma_3 > \sigma_\psi \end{cases}$$

Window 2-4

Window 2-5: Flow rule for Rankine mechanism

ZSoil®

The flow vector for Rankine mechanism, expressed in the principal axes, is defined as follows

$$\begin{aligned} r_1^R &= 0 \\ r_2^R &= 0 \\ r_3^R &= -1 \end{aligned}$$

Window 2-5

2.4 Strain hardening and softening laws

Window 2-6: Standard hardening law

ZSoil®

The pre-peak hardening can be reproduced by means of plastic strain dependent HB parameters $a(\gamma^p)$, $s(\gamma^p)$ and $m_b(\gamma^p)$. To distinguish whether the hardening, softening or the residual phase is followed the two limits of the plastic deviatoric strain γ^p must be specified i.e. the γ^r and γ^{res} (γ^{res} ¿ γ^r). The elastic phase corresponds to $\gamma^p \leq 0$, pre-peak phase to $0 < \gamma^p \leq \gamma^r$, post-peak to $\gamma^r < \gamma^p \leq \gamma^{res}$ and residual phase for $\gamma^p > \gamma^{res}$.

In the pre-peak phase all parameters $a(\gamma^p)$, $s(\gamma^p)$ and $m_b(\gamma^p)$ are assumed to be linear functions of γ^p (the a, s, m_b parameters are corresponding to the transition from hardening to softening (peak)).

$$
\begin{aligned}
a(\gamma^p) &= a^o + (a - a^o)\xi \\
s(\gamma^p) &= s^o + (s - s^o)\xi \\
m_b(\gamma^p) &= m_b^o + (m_b - m_b^o)\xi \\
\xi &= \frac{\gamma^p}{\gamma^r} \\
\gamma^p &= \int \sqrt{\frac{2}{3}\dot{\varepsilon}_{ij}^{p,HB}\dot{\varepsilon}_{ij}^{p,HB}}\,\mathrm{d}t
\end{aligned}
$$

It has to be emphasized here that the equivalent deviatoric plastic strain used in the above hardening law is produced only by the HB mechanism.

This law generates the following shape of $q - \varepsilon_1$ curve in the triaxial tests (here consider hardening branch only) that may deviate from the one observed in the experiment.

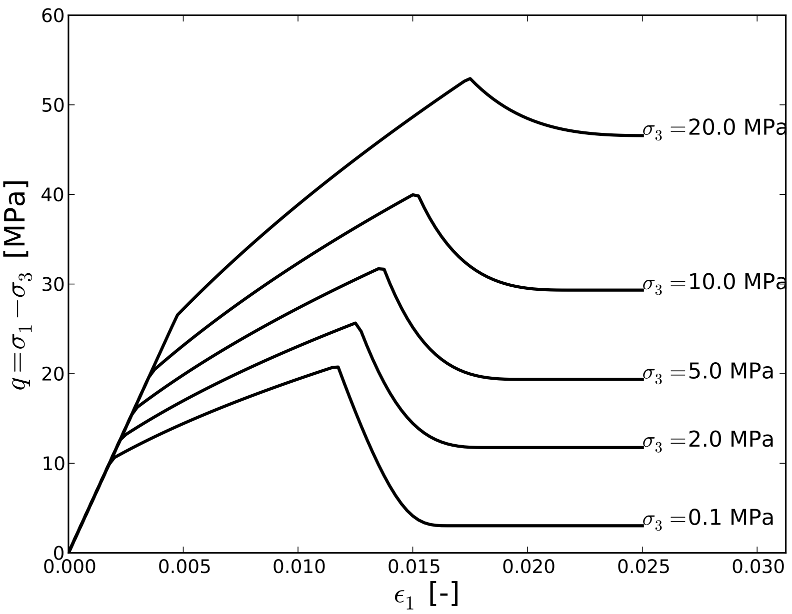

Typical shape of $q - \varepsilon_1$ curve in the triaxial test obtained for standard hardening law

Window 2-6

Window 2-7: Setting parameters for standard hardening law

ZSoil®

In order to avoid spurious model behavior, when standard hardening law is used (part of the initial yield envelope is outside peak one), one has to fulfill the following condition for any value of the σ_3 stress.

$$\left(m_b^o \frac{\sigma_3}{\sigma_{ci}} + s^o\right)^{a^o} < \left(m_b \frac{\sigma_3}{\sigma_{ci}} + s\right)^a$$

For $a^o = a$ the above conditions will always be satisfied if

$$\begin{aligned} m_b^o &\leq m_b \\ s^o &\leq s \end{aligned}$$

It is therefore recommended to assume $a_o = a$.

Another condition that should also be fulfilled is such that the absolute value of the initial uniaxial/biaxial tensile strength should be smaller than, or equal to, absolute value of the peak one. This condition is as follows

$$\frac{s_o}{m_{bo}} \leq \frac{s}{m_b}$$

Window 2-7

Window 2-8: Parabolic hardening law

ZSoil®

Different forms of the hardening law can be obtained by rewriting the HB criterion in the following manner

$$f(\sigma_1, \sigma_3) = \sigma_1 - \sigma_3 - \sigma_{ci} \left(m_b \frac{\sigma_3}{\sigma_{ci}} + s\right)^a \left\{(r(\xi))^{1/a}\right\}^a$$

where $r(\xi)$ is an assumed hardening function and $\xi = \dfrac{\gamma^p}{\gamma^r}$. **It has to be emphasized here that the equivalent deviatoric plastic strain used in the above hardening law is produced only by the HB mechanism**.

The analytical form of $r(\xi)$ function, assumed here as 4-th order parabola, is as follows

$$r(\xi) = 1 - (1 - r_o)(1 - \xi)^4$$

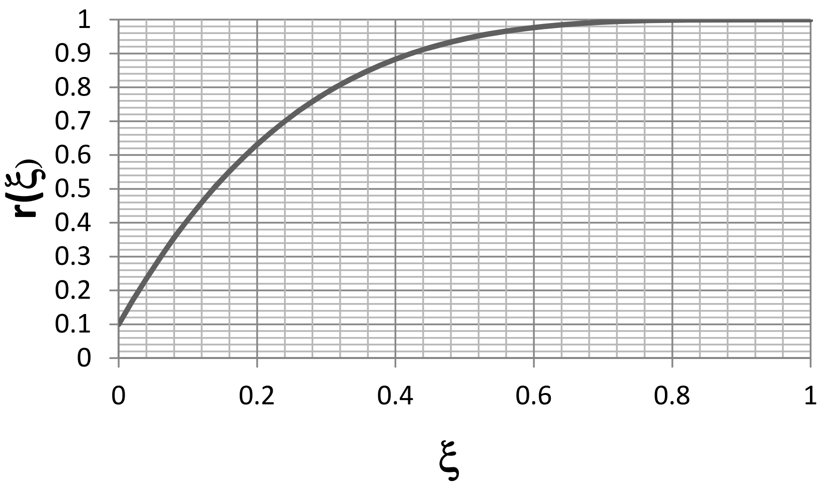

Evolution of the hardening function $r(\xi)$

It is worth to note that the above hardening form yields the following m_{bo} and s_o parameters (this way the biaxial tensile strength remains constant during hardening that is not the case for the standard hardening law)

$$
\begin{aligned}
m_{bo} &= m_b \, r(\xi)^{1/a} \\
s_o &= s \, r(\xi)^{1/a}
\end{aligned}
$$

This law generates the following shape of $q - \varepsilon_1$ curve in the triaxial tests (here consider hardening branch only) that may represent the experiment in a much better way than the standard one.

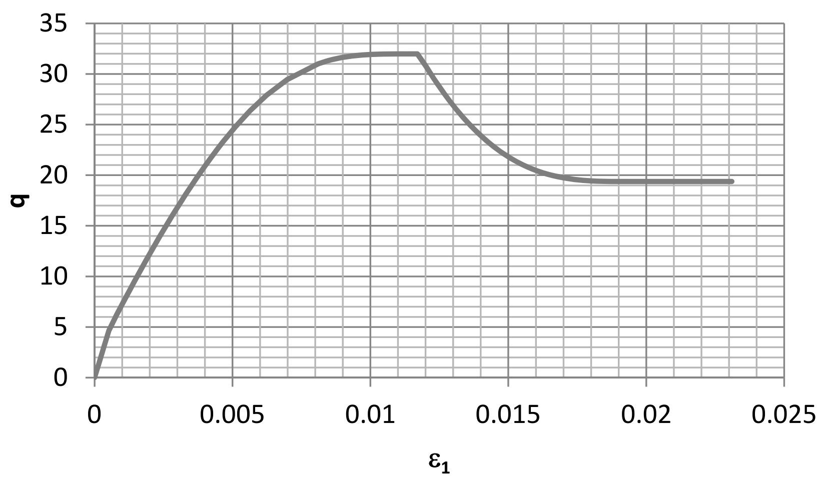

Typical shape of $q - \varepsilon_1$ curve in the triaxial test obtained for parabolic hardening law

The only material parameter used in this law is so far the r_o (although one could also add power value that is fixed to value 4.0). This parameter should fulfill the condition

$$r_{o,min} \leq r_o < 1.0$$

and $r_{o,min} \geq 10^{-4}$.

Window 2-8

Window 2-9: Hardening law including stiffening effect

ZSoil®

Another useful form of the hardening law can be obtained assuming more complex form of the $r(\xi)$ function (see figure below). It consists of three segments i.e. the linear one for $\xi < \xi_1$, 3-rd order parabola for $\xi_1 \leq \xi \leq \xi_2$ and 4-th order parabola for $\xi > \xi_2$. This curve is designed by four parameters i.e. ξ_1, r_1, ξ_2 and r_2. The proposed curve is smooth and preserves continuity up to first derivatives with respect to ξ at the two characteristic points.

The linear branch (first segment) of the hardening law is described by the following equation

$$r(\xi) = \frac{\xi}{\xi_1}\, r_1$$

The third range approximated by 4-th order parabola is defined as follows

$$\begin{aligned} r(\xi) &= 1 - B_1\, (1-\xi)^4 \\ B_1 &= \frac{(1-r_2)}{(1-\xi_2)^4} \end{aligned}$$

The second branch approximated by 3-rd order parabola is defined by the following expression

$$r(\xi) = A_1 + A_2\xi + A_3\xi^2 + A_4\xi^3$$

The A_1, A_2, A_3, A_4 coefficients are computed by solving set of linear equations (these equations express continuity of $r(\xi)$, and its derivative, at points (ξ_1, r_1), (ξ_2, r_2)

$$\begin{aligned} A_4\xi_1^3 + A_3\xi_1^2 + A_2\xi_1 + A1 &= r_1 \\ 3\ A_4\ \xi_1^2 + 2\ A_3\ \xi_1 + A_2 &= \frac{r_1}{\xi_1} \\ A_4\ \xi_2^3 + A_3\ \xi_2^2 + A_2\xi_2 + A_1 &= r_2 \\ 3\ A_4\xi_2^2 + 2\ A_3\xi_2 + A_2 &= \frac{4\ (1-r2)}{(1-\xi_2)} \end{aligned}$$

The analytical formulas for polynomial A_1, A_2, A_3, A_4 are not given here due to their complexity (these are computed internaly in the calculation module).

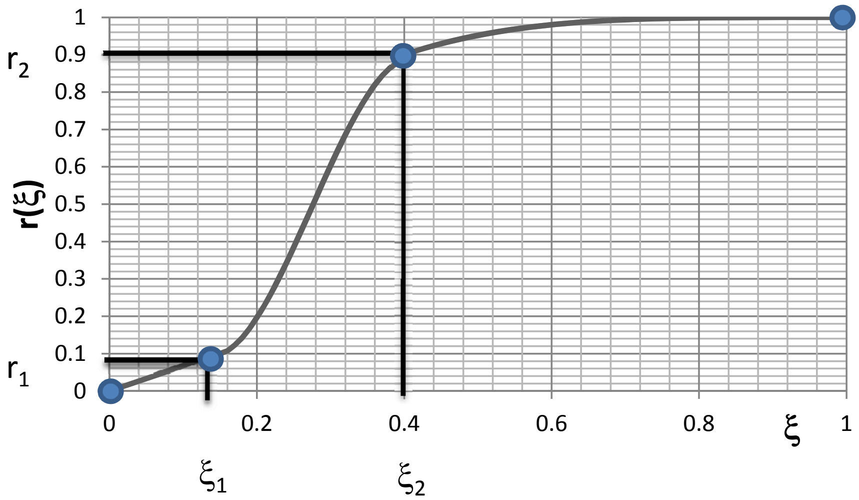

Evolution of the hardening function $r(\xi)$

This law generates the following shape of $q - \varepsilon_1$ curve in the triaxial tests (here consider hardening branch only) that may represent the effect of stiffening observed at the begining of the experiment (see experimental results given in section 4.3) .

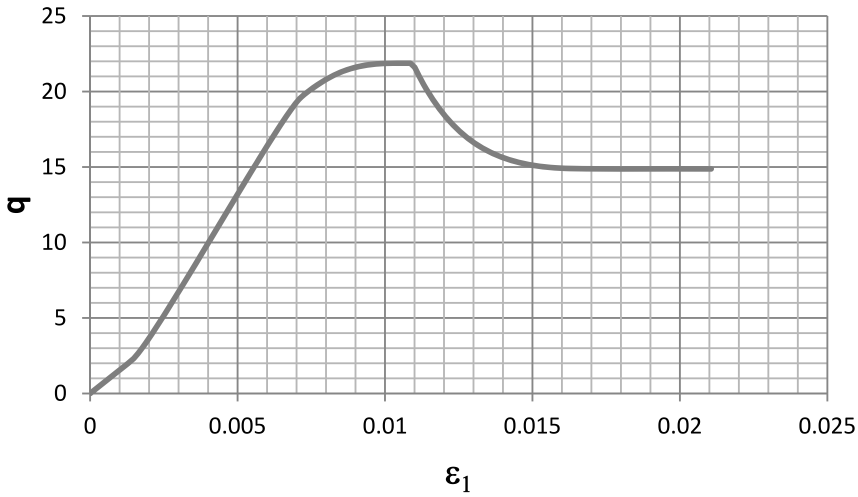

Typical shape of $q - \varepsilon_1$ curve in the triaxial test obtained for hardening law with stiffening effect

The ξ_1, r_1, ξ_2 and r_2 parameters must fulfil the folowing conditions

$$0 < r_1 < r_2 < 1$$
$$0 < \xi_1 < \xi_2 < 1$$

Window 2-9

Window 2-10: Softening for HB mechanism

ZSoil®

The post-peak softening phenomenona can be reproduced by means of plastic strain dependent HB parameters $a(\gamma^p)$, $s(\gamma^p)$ and $m_b(\gamma^p)$. To distinguish whether the hardening, softening or the residual phase is followed the two limits of the plastic deviatoric strain γ^p must be specified i.e. the γ^r and γ^{res} (γ^{res} ¿ γ^r). The elastic phase corresponds to $\gamma^p \leq 0$, pre-peak phase to $0 < \gamma^p \leq \gamma^r$, post-peak to $\gamma^r < \gamma^p \leq \gamma^{res}$ and residual phase for $\gamma^p > \gamma^{res}$.

In the post-peak phase all parameters $a(\gamma^p)$, $s(\gamma^p)$ and $m_b(\gamma^p)$ are assumed to be 3-rd order polynomial functions of γ^p (the a, s, m_b parameters are corresponding to the transition from hardening to softening (peak)).

$$
\begin{aligned}
a(\gamma^p) &= a^{res} + (a - a^{res})\,(1-\xi_2)^3 \\
s(\gamma^p) &= s^{res} + (s - s^{res})\,(1-\xi_2)^3 \\
m_b(\gamma^p) &= m_b^{res} + (m_b - m_b^{res})\,(1-\xi_2)^3 \\
\xi_2 &= \frac{\gamma^p - \gamma^r}{\gamma^{res} - \gamma^r}
\end{aligned}
$$

For $\gamma^p > \gamma^{res}$ residual values are kept.

Triaxial experiments show a vanishing effect of softening behavior for larger values of the confining stress σ_3. In order to capture that effect one may specify the cut-off σ_{sf} stress that cancels softening. To include that effect in the model we assume that any of the residual value of parameters a^{res}, m_b^{res} or s^{res}, is defined as

$$
\begin{aligned}
a^{res} &= a_o^{res} + (a - a_o^{res})\,(1 - f_{\sigma_s}(\sigma_3)) \\
s^{res} &= s_o^{res} + (s - s_o^{res})\,(1 - f_{\sigma_s}(\sigma_3)) \\
m_b^{res} &= m_{bo}^{res} + (m_b - m_{bo}^{res})\,(1 - f_{\sigma_s}(\sigma_3))
\end{aligned}
$$

To avoid sudden switch from strong softening to ideal plasticity an arbitrary (piecewise linear) function $f_{\sigma_s}(\sigma_3)$ is introduced in the above expressions. It takes the following form

$$
\begin{aligned}
f_{\sigma_s}(\sigma_3) &= 1 - \frac{\sigma_3}{\sigma_{sf}} \quad \text{for } 0 \leq \sigma_3 \leq \sigma_{sf} \\
f_{\sigma_s}(\sigma_3) &= 1 \quad \text{for } \sigma_3 < 0 \\
f_{\sigma_s}(\sigma_3) &= 0 \quad \text{for } \sigma_3 > \sigma_{sf}
\end{aligned}
$$

Window 2-10

Window 2-11: Setting parameters for HB softening law

ZSoil®

In order to avoid spurious model behavior one has to fulfill the following condition for any value of the σ_3 stress.

$$\left(m_b \frac{\sigma_3}{\sigma_{ci}} + s\right)^a > \left(m_{bo}^{res} \frac{\sigma_3}{\sigma_{ci}} + s_o^{res}\right)^{a_o^{res}}$$

For $a_o^{res} = a$ the above conditions will always be satisfied if

$$\begin{aligned} m_b^{res} &\leq m_b \\ s_o^{res} &\leq s \end{aligned}$$

The next condition that should also be fulfilled is such that the residual uniaxial/biaxial tensile strength should be smaller or equal to the peak one. This condition is as follows

$$\frac{s_{res}}{m_{res}} \leq \frac{s}{m_b}$$

Another limitation that must be put on γ^{res} value can be derived from plastic consistency condition written for an unconfined compression test at the beginning of the softening branch (at this point tangent to the $\sigma - \varepsilon$ curve is the steepest). This condition derived from inequality $\frac{\partial F}{\partial \sigma_i} D_{ij}^e \, r_j + H > 0$ (H is a plastic modulus) yields the following formula for the minimal value of the residual plastic strain γ^{res}.

$$\gamma^{res} \geq \gamma^r + \frac{3\sigma_{ci} \; s^a \; a \, (s - s^{res})}{4Gs + 2 \; s^a \; a \; m_b \, (G \, (1 + \sin\psi) + \lambda \sin\psi)}$$

The worst possible case is for $\sin\psi = 0$ that will usually happen when strain dependent dilatancy is activated and ψ multiplier at $\gamma = \gamma^r$ is equal to zero.

Window 2-11

Window 2-12: Softening for Rankine mechanism

ZSoil®

Softening law for the Rankine criterion is applied to the f_t parameter using the following expression

$$f_t(w) = f_{to} \left(\frac{\min\left(|\sigma_t^{HB}|, |\sigma_{t,peak}^{HB}|\right)}{|\sigma_{t,peak}^{HB}|} \right) \; e^{-\alpha^R \, w}$$

where f_{to} is the peak uniaxial tensile strength defined for Rankine mechanism, σ_t^{HB} and $\sigma_{t,peak}^{HB}$ are the current and peak biaxial tensile strengths induced by the HB criterion, while w is defined as follows

$$w = -\int \dot{\varepsilon}_3^R \mathrm{d}t$$

and $\dot{\varepsilon}_3^R$ is the value of the largest tensile plastic strain induced by the Rankine mechanism only. The standard hardening as well as the softening law influence the current value of biaxial and uniaxial tensile strengths. Therefore to avoid singular situations the extra scaling term $\frac{\min\left(|\sigma_t^{HB}|, |\sigma_{t,peak}^{HB}|\right)}{|\sigma_{t,peak}^{HB}|}$ is added to the softening rule for the Rankine criterion. There only restriction that must be preserved concerns the s^{res}. Its value must satisfy the condition

$$s^{res} > 0$$

The above form of the softening law leads to the weakly coupled shear and tensile plastic mechanism. The shear mechanism influences the current value of the tensile strength while tensile mechanism does not influence the compressive strength.

Window 2-12

2.5 Regularization techniques for strain softening

To circumvent pathological mesh dependency, softening modulus scaling technique is implemented.

Window 2-13: Scaling softening moduli

ZSoil®

To avoid mesh dependency for strain softening models we may use the approach proposed in 1981 by Mróz and Pietruszczak [3]. Let us assume that the experimental width of localization zone is denoted by L_c and an averaged size of the finite element by h_e. Having defined the two quantities we can define softening scaling factor $\eta = \dfrac{h_e}{L_c}$. For HB mechanism this factor is included in the modified $\tilde{\gamma}^{res}$ parameter that is defined as follows:

$$\tilde{\gamma}^{res} = \gamma^r + \frac{\gamma^{res} - \gamma^r}{\eta} \tag{1}$$

This modified $\tilde{\gamma}^{res}$ parameter replaces standard γ^{res} one, and it can be different for each finite element in the mesh. Using this technique the width of localization zone is usually larger than L_c but amount of dissipated energy is the same. Therefore we may expect an objective response of the structure in terms of force-displacement characteristics. **However, it must be emphasized here that the minimal value of $\tilde{\gamma}^{res}$ must still satisfy the condition given in Win.2-11**. Hence design of the finite element mesh, in zones where we may expect strong softening behavior, must take that fact into account.

For pure Rankine mechanism the fracture energy G_f should be equal to

$$G_f = \frac{f_{to}\, L_c}{\alpha^R} \tag{2}$$

As the localization will take place in a single element and its size is usually larger than L_c we will need to scale α^R parameter as follows

$$\tilde{\alpha}^R = \eta\, \alpha_R \tag{3}$$

Window 2-13

Chapter 3

Setting material properties

All material properties for HB model are kept in several groups as for any other constitutive model implemented in ZSoil. In this chapter we will discuss those kept in group *Elastic* and *Nonlinear*.

Window 3-1: Elastic properties

ZSoil®

Data group	Parameter	Unit	Default value	Description
Elastic	E	[kN/m^2]	-	Young modulus; can be computed based on given GSI index; for $\sigma_{ci} < 100$ MPa
	ν		0.3	Poisson ratio

Modulus of deformation E can be estimated based on given GSI index by using the following empirical expressions

$$
\begin{aligned}
E[\text{GPa}] &= \left(1 - \frac{D}{2}\right)\sqrt{\frac{\sigma_{ci}}{100}}\; 10^{\left(\dfrac{GSI-10}{40}\right)} \quad \text{for} \quad \sigma_{ci} \leq 100 \text{ MPa} \\
E[\text{GPa}] &= \left(1 - \frac{D}{2}\right)\; 10^{\left(\dfrac{GSI-10}{40}\right)} \quad \text{for} \quad \sigma_{ci} > 100 \text{ MPa}
\end{aligned}
$$

Window 3-1

Window 3-2: Properties specific to HB model

ZSoil®

Material properties specific to HB model are kept in four subgroups related to

1. HB yield criterion **(A)**
2. Dilatancy law **(B)**
3. Hardening **(C)**
4. Softening **(D)**

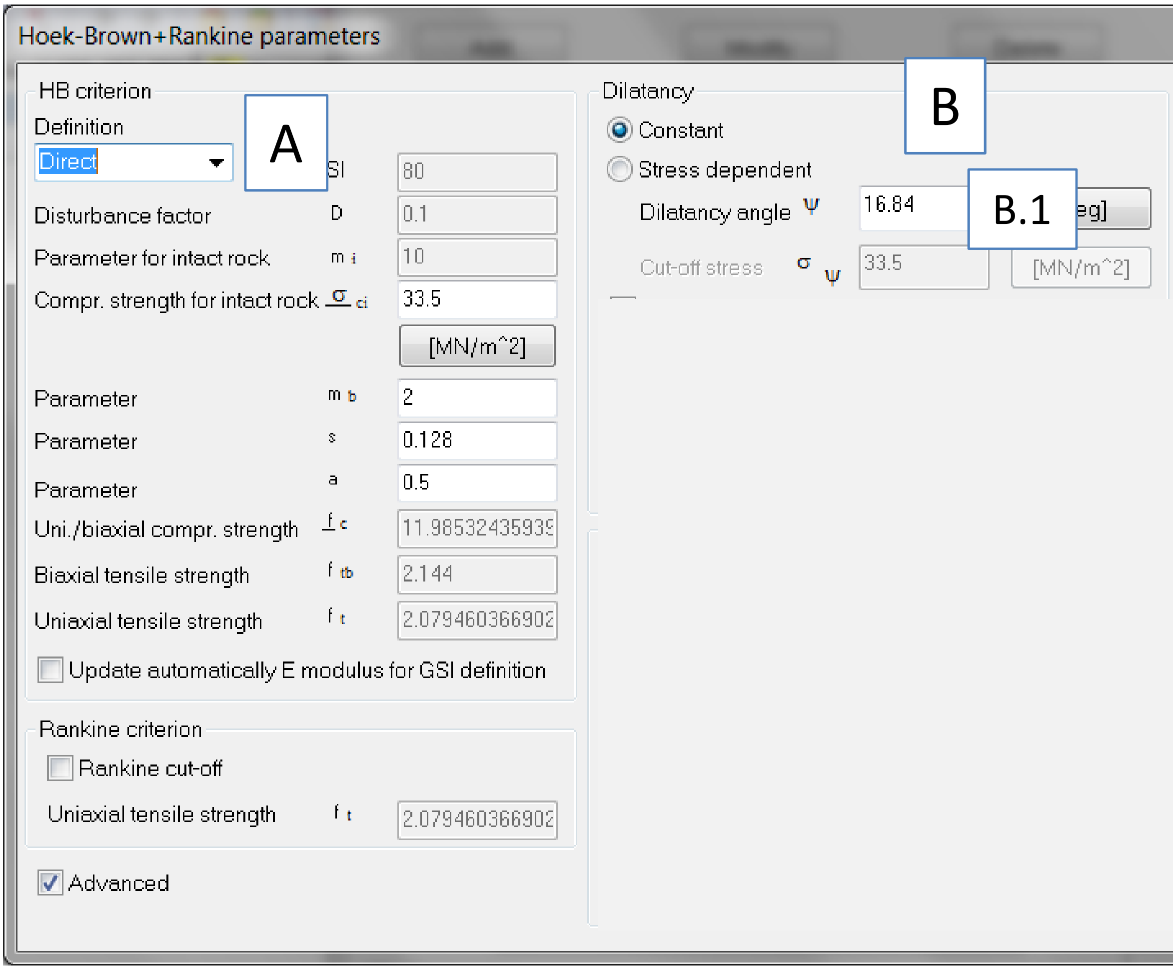

User interface for properties in group *Nonlinear*

Window 3-2

Window 3-3: Properties specific to HB model

ZSoil®

Subgroup	Parameter	Unit	Range	Description
HB criterion	Definition	[-]	**Direct, GSI**	For Direct user must set σ_{ci}, m_b, s and a values; For GSI user must set GSI, D,m_i and σ_{ci} values
	GSI	[-]	0 ÷ 100	GSI value
	D	[-]	0 ÷ 1	Disturbance factor; for undisturbed rock mass D=0.0 while for highly disturbed ones D =1.0 (active only for GSI definition)
	m_i	[-]	> 0	Ratio $\frac{\lvert f_t \rvert}{f_c}$ for intact rock (default is 10.0) (active only for GSI definition)
	σ_{ci}	[kPa]	> 0	Compressive strength of intact rock
	m_b	[-]	$> m_i$	Same meaning as m_i but for rock mass (active only for Direct definition)
	s	[-]	0 ÷ 1	Responsible for ductility of rock mass (active only for Direct definition)
	a	[-]	0.5 ÷ 0.67	Responsible for curvature of HB line in $q-\sigma_3$ axes (active only for Direct definition)
	☒ **Update E**		ON/OFF	Logical flag indicating that E modulus will be recomputed based on given GSI index using empirical formula (active only for GSI definition)
Rankine criterion	☒ **Rankine cut-off**		ON/OFF	Flag for Rankine cut-off activation (it will be activated internally at value of the uniaxial tensile strength f_t^{HB} if set OFF)
	$\lvert f_t \rvert$	[kPa]	$0 \leq \lvert f_t \rvert \leq \lvert f_t^{HB} \rvert$	Assumed uniaxial tensile strength
Dilatancy	Type		⊚ **Constant** ⊚ **Stress dep.**	User may select constant or stress dependent dilatancy law
	ψ	[deg]	≥ 0	Value of dilatancy angle
	σ_ψ	[kPa]	> 0	σ_3 value at which dilatancy is canceled (valid for stress dependent dilatancy option)

	☒ **Strain dep.dil.**		ON/OFF	Flag for strain dependent dilatancy
	f_ψ^o	[-]	default is 0.0	Scaling factor for dilatancy angle during hardening set at $\gamma^p = 0$ (active only when ☒ **Pre-peak hard.** is ON)
	f_ψ^r	[-]	default is 0.0	Scaling factor for dilatancy angle at transition from pre-peak to post-peak state set at $\gamma^p = \gamma^r$ (value 0.0 is recommended)
	f_ψ^{res}	[-]	default is 1.0	Scaling factor for dilatancy angle at transition from post-peak to residual state set at $\gamma^p = \gamma^{res}$ (value 1.0 is recommended)
Hardening	☒ **Pre-peak hard.**		ON/OFF	Flag for pre-peak hardening
	type			can be; *Standard* , *Parabolic or Stiffening*
	γ_r	[-]	> 0	Plastic deviatoric strain at peak of triaxial $q - \varepsilon_1$ curve
Hardening *Standard*	m_b^o	[-]	$\leq m_b$	m_b parameter for pre-peak hardening (active only when ☒ **Pre-peak hard.** is ON)
	s^o	[-]	$\leq s$	s parameter for pre-peak hardening (active only when ☒ **Pre-peak hard.** is ON)
	a^o	[-]	$\leq a$	a parameter for pre-peak hardening (active only when ☒ **Pre-peak hard.** is ON)
Hardening *Parabolic*	r_o	[-]	$0 < r_o < 1$	Fraction of q/q_f at which switch from linear elastic to elasto-plastic hardening will occur (active only when ☒ **Pre-peak hard.** is ON)
Hardening with *Stiffening*	ξ_1	[-]	$0 < \xi_1 < \xi_2 < 1$	Value of γ^p/γ^r at which stiffening effect starts to occur (active only when ☒ **Pre-peak hard.** is ON)
	r_1	[-]	$0 < r_1 < r_2 < 1$	Value of hardening function $r(\xi_1)$ (active only when ☒ **Pre-peak hard.** is ON)

	ξ_2	[-]	$0 < \xi_1 < \xi_2 < 1$	Value of γ^p/γ^r at transition point on $r(\xi)$ curve where transition point from third order parabola to 4-th order one occurs (active only when ☒ **Pre-peak hard.** is ON)
	r_2	[-]	$0 < r_1 < r_2 < 1$	Value of hardening function $r(\xi_2)$ (active only when ☒ **Pre-peak hard.** is ON)
Softening	☒ **Post-peak soft.**		ON/OFF	Flag for post-peak softening
	γ_{res}	[-]	$> \gamma_r$	Plastic deviatoric strain at residual state on triaxial $q - \varepsilon_1$ curve
	m_{bo}^{res}	[-]	$\leq m_b$	m_b parameter for post-peak softening (active only when ☒ **Post-peak soft.** is ON)
	s_o^{res}	[-]	$\leq s$	s parameter for post-peak softening (active only when ☒ **Post-peak soft.** is ON)
	a_o^{res}	[-]	$\leq a$	a parameter for post-peak softening (active only when ☒ **Post-peak soft.** is ON)
	σ_{sf}	[kPa]	> 0	Value of σ_3 at which softening is cancelled (smoothly)
	Type of regularization		Local / Softening scaling	Choice of softening regularization method (Local means no regularization)
	Char.length	[m]	> 0	Characteristic length is used to adjust the amount of fracture energy under tension and compression

Window 3-3

Window 3-4: Recommendations for setting HB properties

ZSoil®

In order to keep full control of model behavior it is recommended to assume $a_o = a_o^{res} = a$. If a parameter is close to 0.5 then it recommended to use a strict value $a = 0.5$ because this may reduce the computational effort in stress return algorithm (stress return can be solved in an exact manner). If the pre-peak hardening is activated the two parameters s^o and m_b^o have to be set. One may use the uniaxial compression test to identify the fraction of the peak compressive strength at which hardening is well visible (let say $\eta = 0.5$).

Then s^o can easily be computed as $s^o = s \quad \eta^{1/a}$ (for $s = 1$, $\eta = 0.5$ and $a = 0.5$ the resulting $s^o = 1 * 0.5^2 = 0.25$). The m_b^o parameter must be optimized or one may require that in the tensile test the biaxial tensile strength resulting from the HB criterion remains unchanged. This can be achieved assuming $m_b^o = m_b \dfrac{s^o}{s}$. The m_b, s and a parameters can be obtained from empirical correlations based on GSI index but they can directly be obtained from optimization procedure based on peak deviatoric stresses reached in triaxial tests (run under constant σ_3 confining stresses) and assumed value of intact rock compressive strength σ_{ci}. The m_{bo}^{res} and s_o^{res} parameters (if $a = a^o = a_o^{res}$) can be obtained from optimization procedure based on residual deviatoric stresses reached in triaxial tests.

Window 3-4

Chapter 4

Benchmarks

4.1 Triaxial test for standard HB model and constant dilatancy

Files: HB-triax-std-dil-const-sig3-0MPa.inp, HB-triax-std-dil-const-sig3-2MPa.inp, HB-triax-std-dil-const-sig3-5MPa.inp

The aim of this benchmark is to reproduce HB failure envelope in the triaxial test run for three different confining stresses σ_3 =0 MPa, σ_3 =2 MPa, σ_3 =5 MPa assuming constant value of dilatancy angle. This benchmark is run as a single finite element test with an imposed vertical displacement (see Figure below). In the initial state vertical fixities are not active and initial isotropic stress state is generated through applied external pressures q equivalent to the given confining stress σ_3. Later on vertical fixities in points A, B are added and test is controlled via imposed displacements.

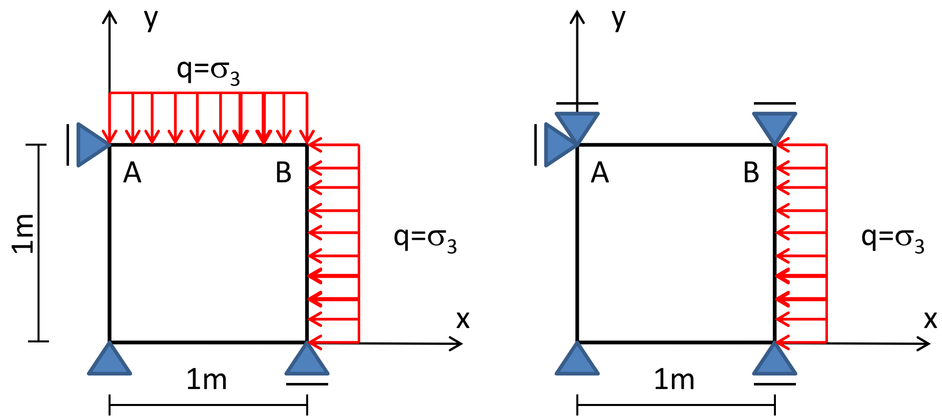

Triaxial test setup

Set of meaningful parameters used in this test is given in the table below.

Group	Subgroup	Parameter	Unit	Value
Elastic		E	[MPa]	26711.2
		ν	[-]	0.3
Nonlinear	HB criterion	Definition		**GSI**

		GSI	[-]	80.0
		D	[-]	0.1
		m_i	[-]	10.0
		σ_{ci}	[MPa]	25.0
		m_b	[-]	4.715
		s	[-]	0.1
		a	[-]	0.5
		☒ **Update E**		Yes
	Rankine criterion	☒ **Rankine cut-off**	[-]	OFF
	Dilatancy	Type		◎ **Constant**
		σ_ψ	[MPa]	unused
		ψ	[deg]	10.0
		☒ **Strain dep.dil.**		OFF
	Hardening	☒ **Pre-peak hard.**		OFF
	Softening	☒ **Post-peak soft.**		OFF

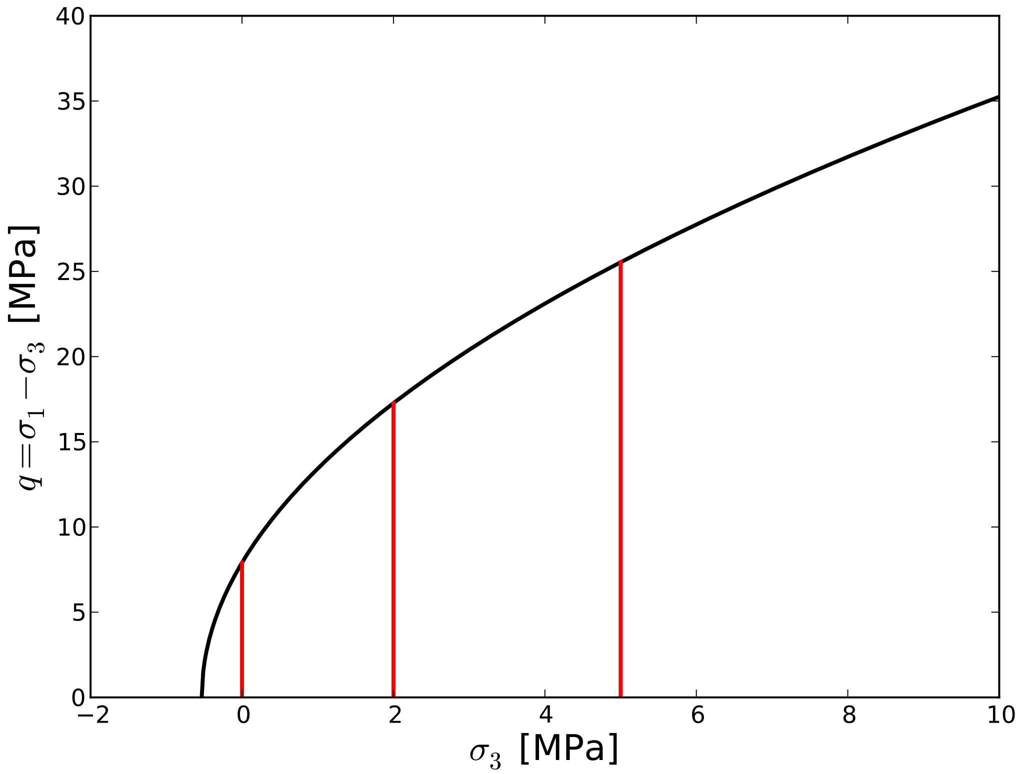

Stress paths in $q - \sigma_3$ axes

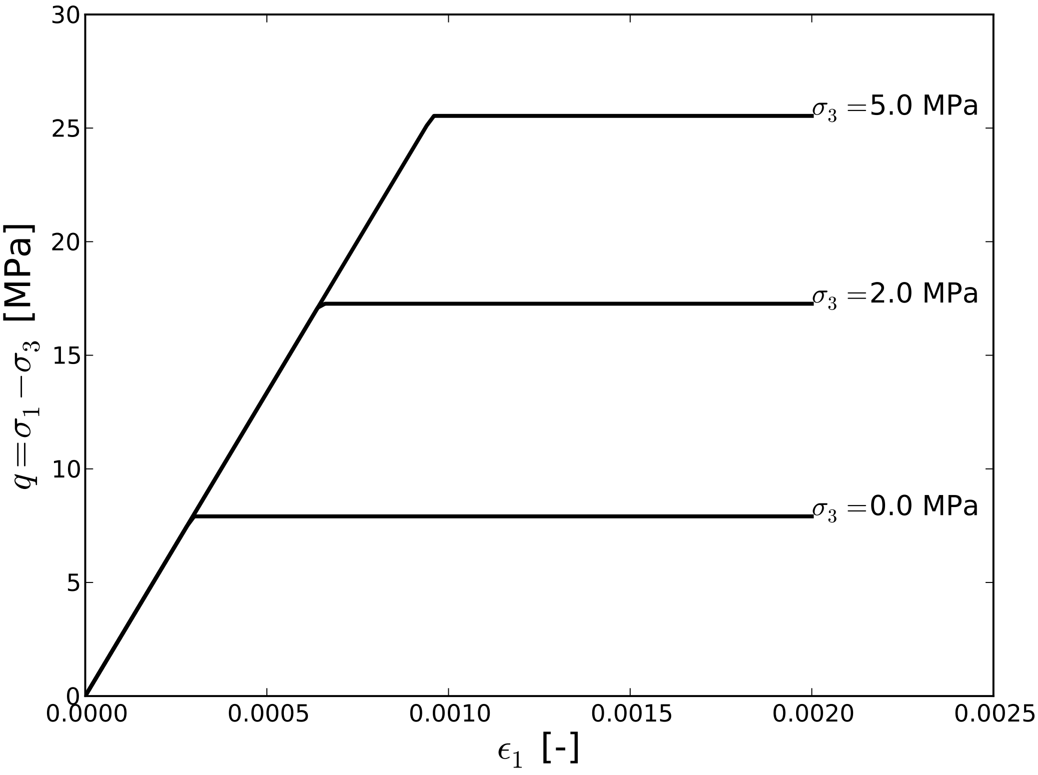

Shear characteristics $q = q(\varepsilon_1)$

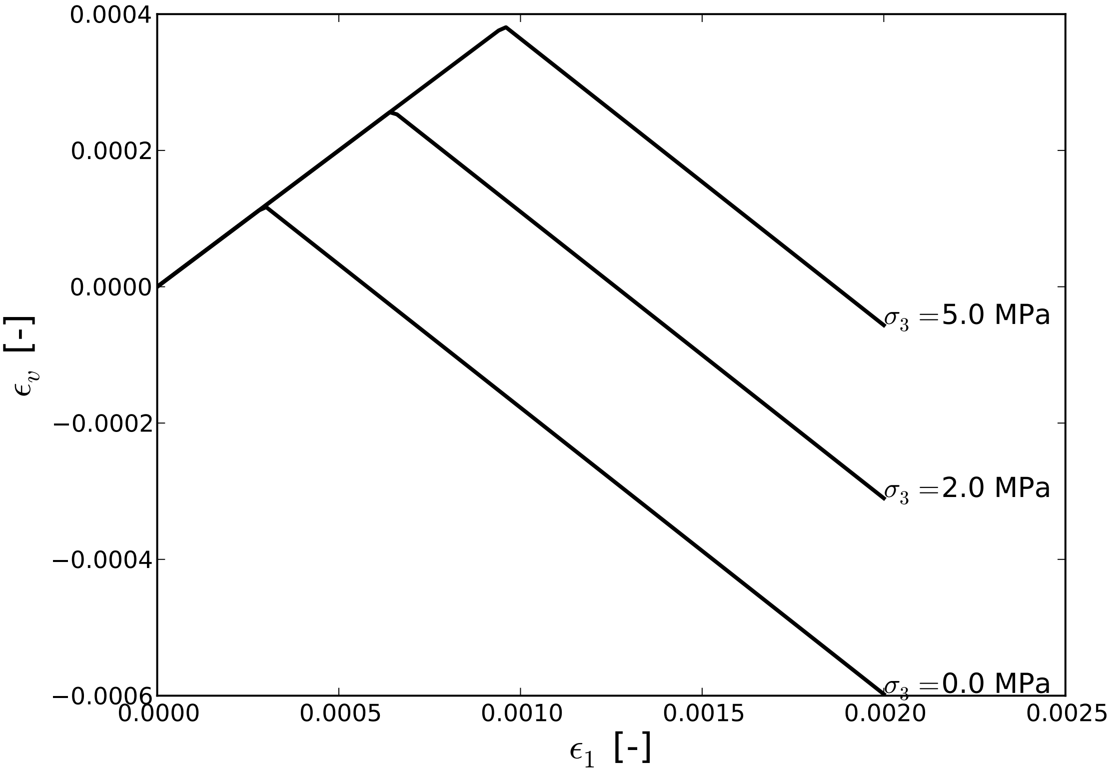

Dilatancy characteristics $\varepsilon_v = \varepsilon_v(\varepsilon_1)$

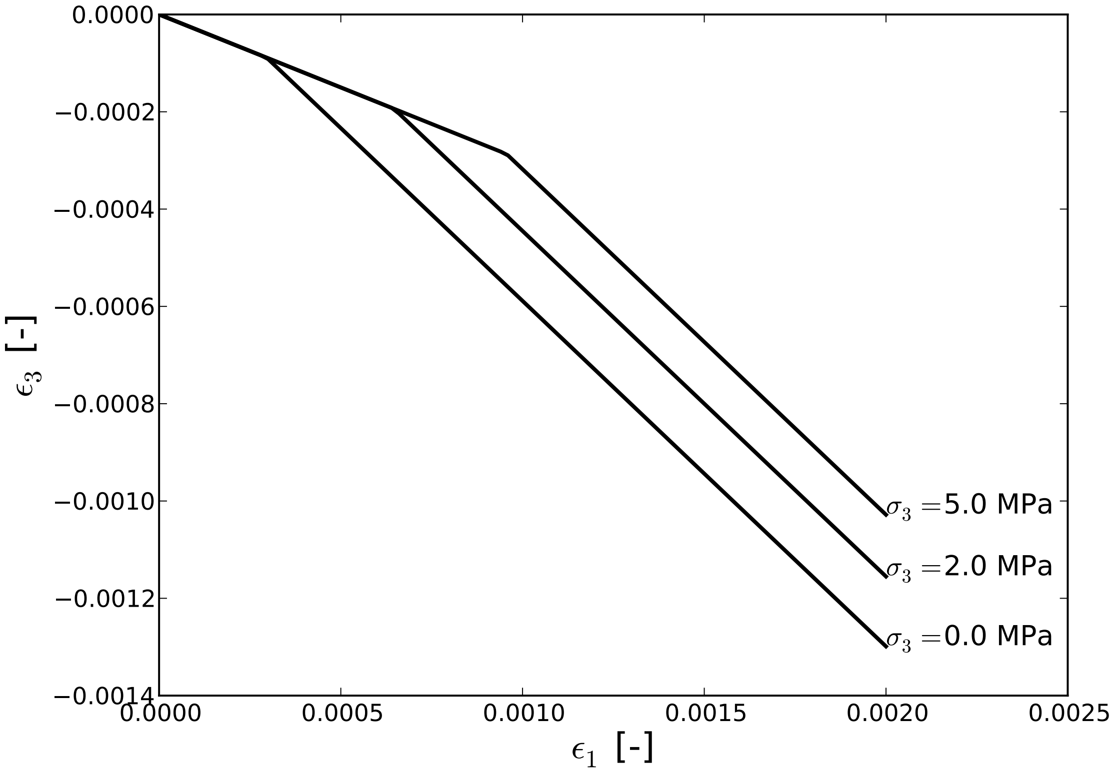

Dilatancy characteristics $\varepsilon_3 = \varepsilon_3(\varepsilon_1)$

4.2 Triaxial test for standard HB model and stress dependent dilatancy

Files: HB-triax-std-dil-var-sig3-0MPa.inp, HB-triax-std-dil-var-sig3-2MPa.inp, HB-triax-std-dil-var-sig3-5MPa.inp

The aim of this benchmark is to reproduce HB failure envelope in the triaxial test run for three different confining stresses σ_3 =0 MPa, σ_3 =2 MPa, σ_3 =5 MPa assuming stress dependent dilatancy. This benchmark is run as a single finite element test with an imposed vertical displacement. Set of meaningful parameters used in this test is given in the table below. Vanishing effect of dilatancy with increasing σ_3 value is well visible in the $\varepsilon_v = \varepsilon_v(\varepsilon_1)$ plot. In this test σ_ψ = 5 MPa hence in the computation with σ_3 = 5MPa no dilatancy is produced during plastic yielding.

Group	Subgroup	Parameter	Unit	Value
Elastic		E	[MPa]	26711.2
		ν	[-]	0.3
Nonlinear	HB criterion	Definition		**GSI**
		GSI	[-]	80.0
		D	[-]	0.1
		m_i	[-]	10.0
		σ_{ci}	[MPa]	25.0

		m_b	[-]	4.715
		s	[-]	0.1
		a	[-]	0.5
		☒ **Update E**		Yes
	Rankine criterion	☒ **Rankine cut-off**		OFF
	Dilatancy	Type		◎ **Stress dep.**
		σ_ψ	[MPa]	5.0
		ψ	[deg]	10.0
		☒ **Strain dep.dil.**		OFF
	Hardening	☒ **Pre-peak hard.**		OFF
	Softening	☒ **Post-peak soft.**		OFF

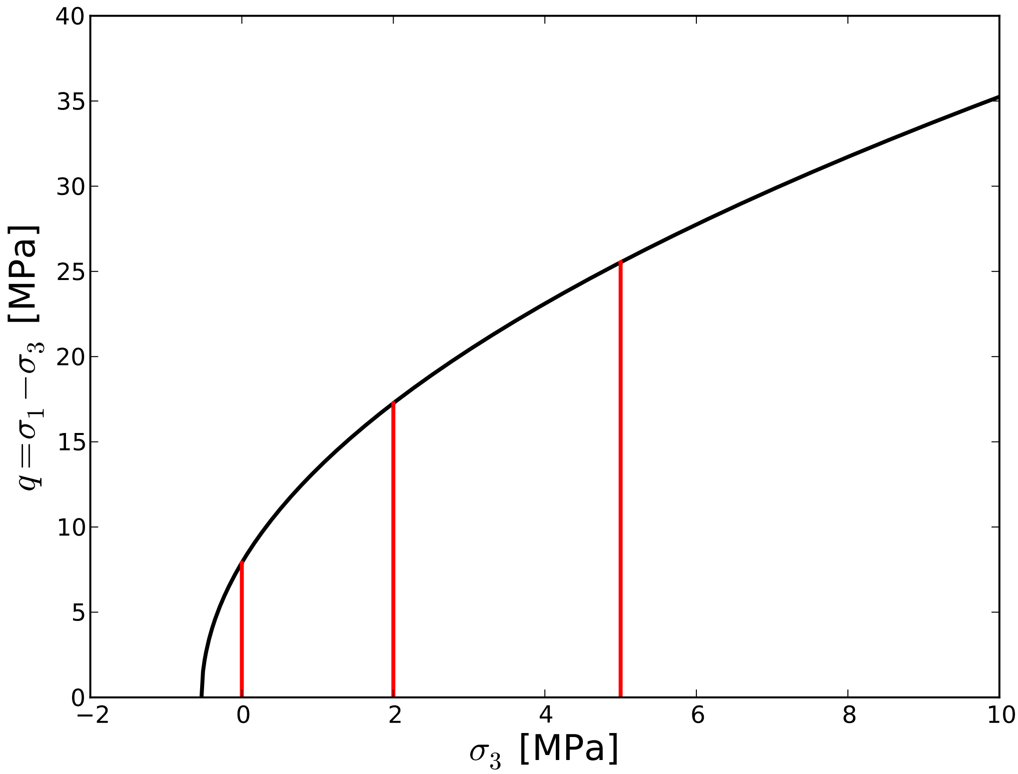

Stress paths in $q - \sigma_3$ axes

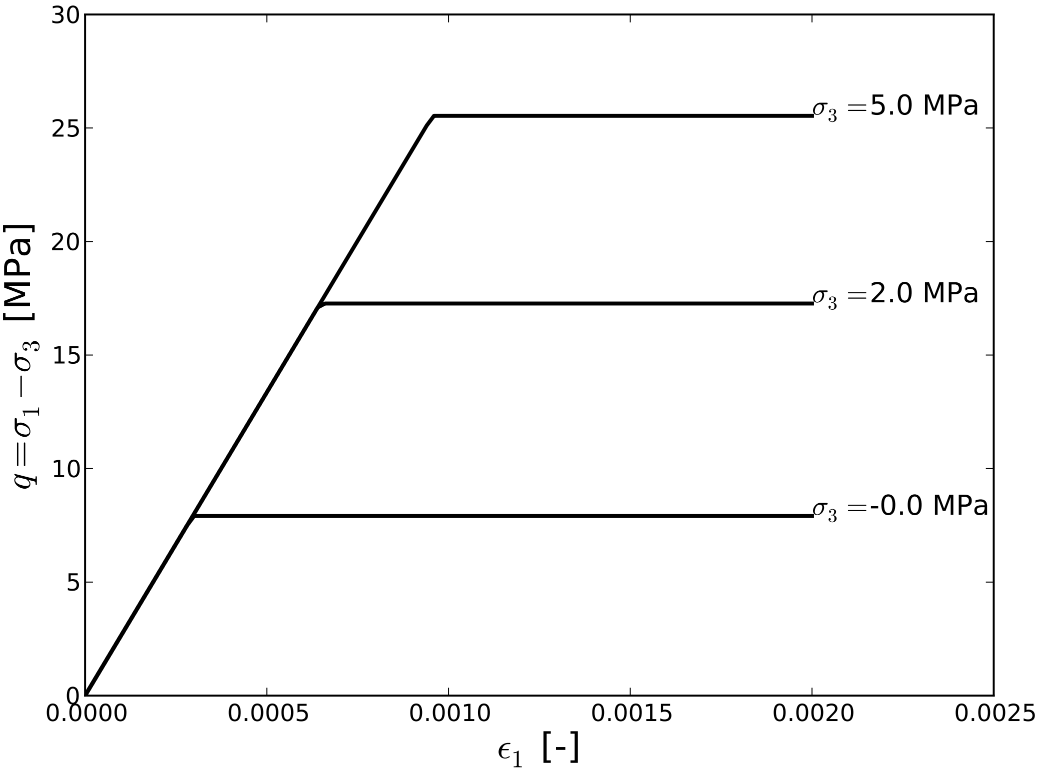

Shear characteristics $q = q(\varepsilon_1)$

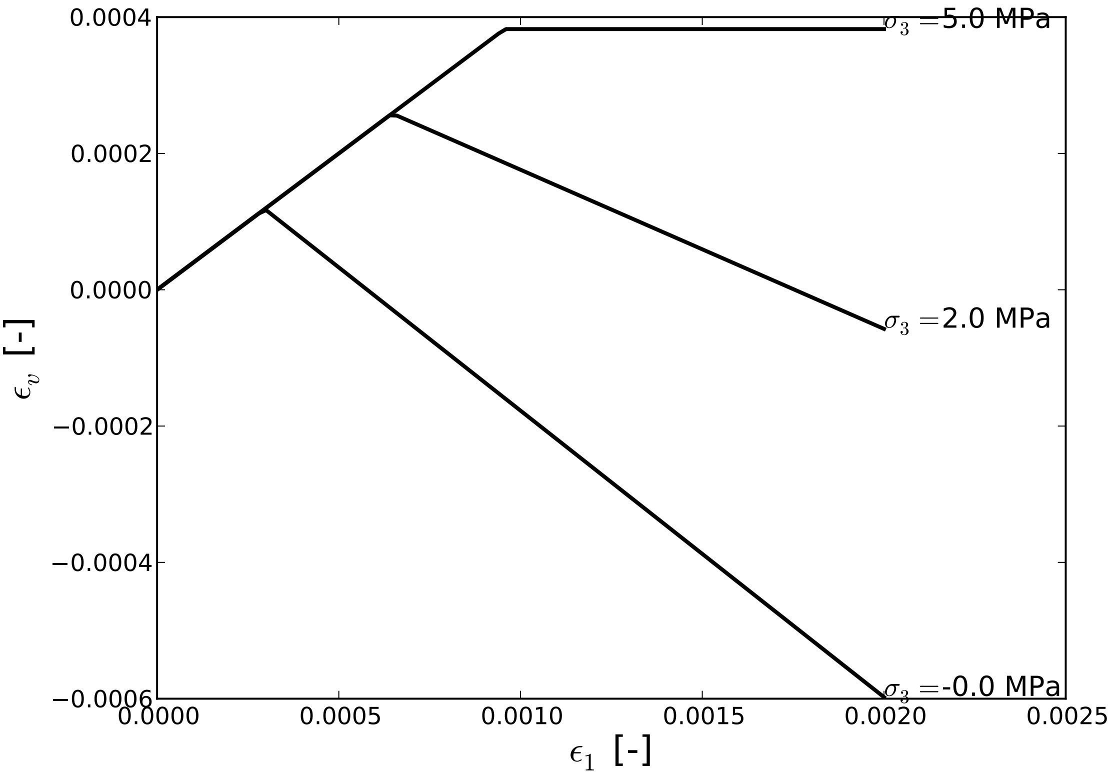

Dilatancy characteristics $\varepsilon_v = \varepsilon_v(\varepsilon_1)$

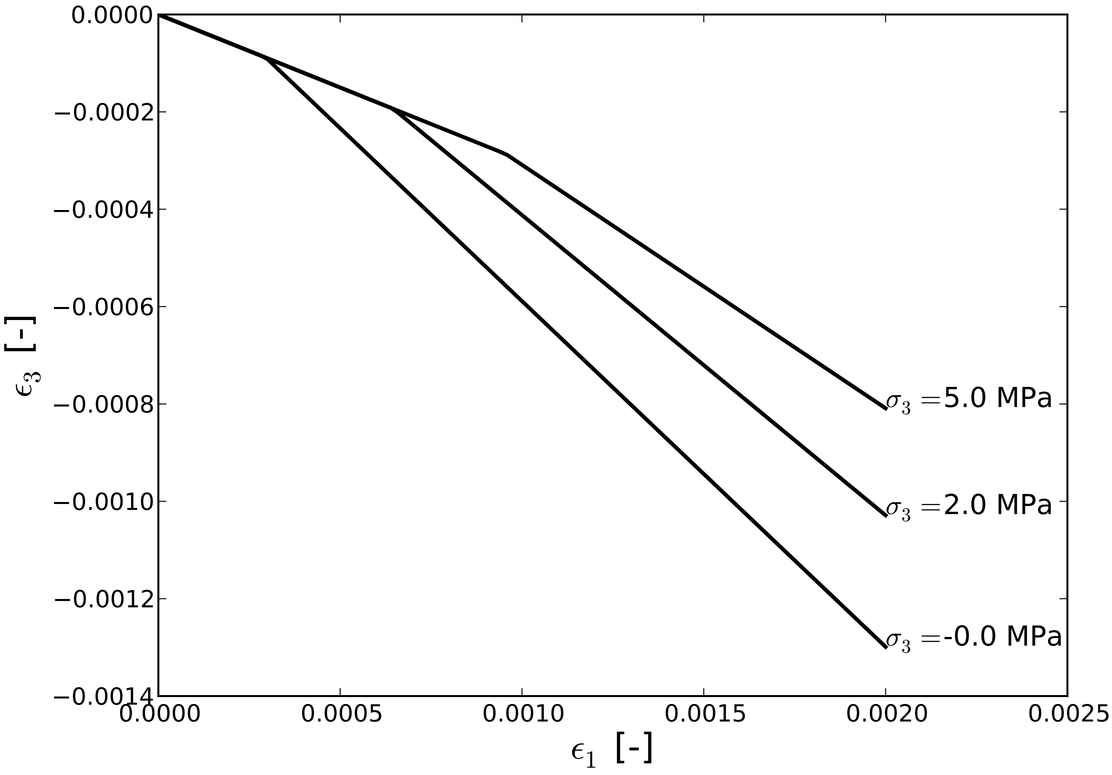

Dilatancy characteristics $\varepsilon_3 = \varepsilon_3(\varepsilon_1)$

4.3 Triaxial test for HB model including pre-peak hardening, post-peak softening and stress/strain dependent dilatancy

Files: HB-triax-hsd-sig3-0_1MPa.inp,HB-triax-hsd-sig3-2MPa.inp, HB-triax-hsd-sig3-5MPa.inp, HB-triax-hsd-sig3-10MPa.inp, HB-triax-hsd-sig3-20MPa.inp

The aim of this benchmark is to reproduce given triaxial test data that was run for five different confining stresses σ_3 =0.1 MPa, σ_3 =2 MPa, σ_3 =5 MPa, σ_3 =10 MPa and σ_3 =20 MPa. In this case pre-peak hardening, post-peak softening and stress /strain dependent dilatancy are taken into account. This benchmark is run as a single finite element test with an imposed vertical displacement. The experimental results are shown in the next two figures [**?**].

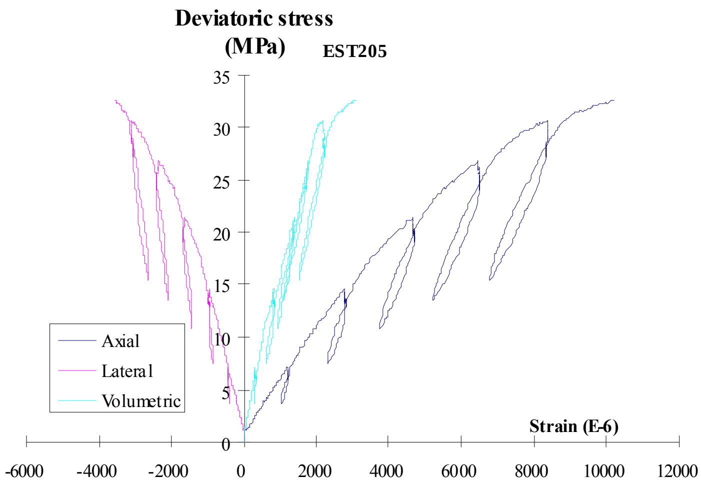

Result for $\sigma_3 = 10$ MPa

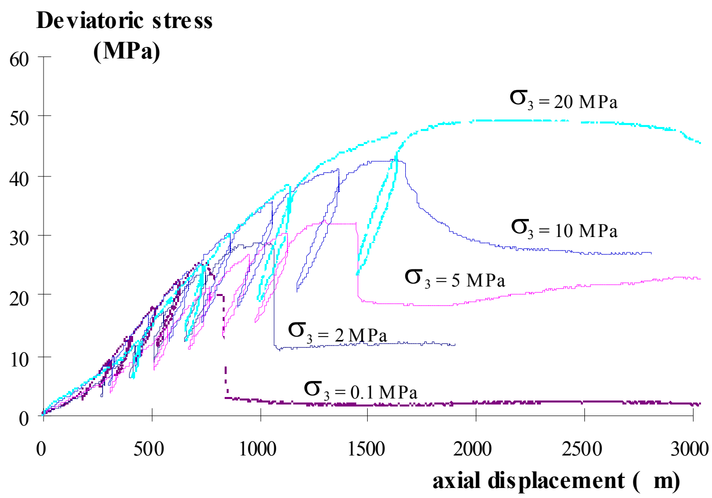

Stress-axial displacement curves

For assumed value of $\sigma_{ci} = 33.5$ MPa parameters m_b, a and s were optimized by minimizing the following error functional F_1

$$
\begin{aligned}
F_1(s, a, m_b) &= \sum_{i=1}^{N=5} \left(1 - \frac{q_f^{peak-theor}(\sigma_{3i})}{q_{fi}^{peak-exp}} \right)^2 \\
q_f^{peak-theor}(\sigma_{3i}) &= \sigma_{ci} \left(m_b \frac{\sigma_3}{\sigma_{ci}} + s \right)^a
\end{aligned}
$$

Result of the optimization procedure and obtained parameters are shown in figure below.

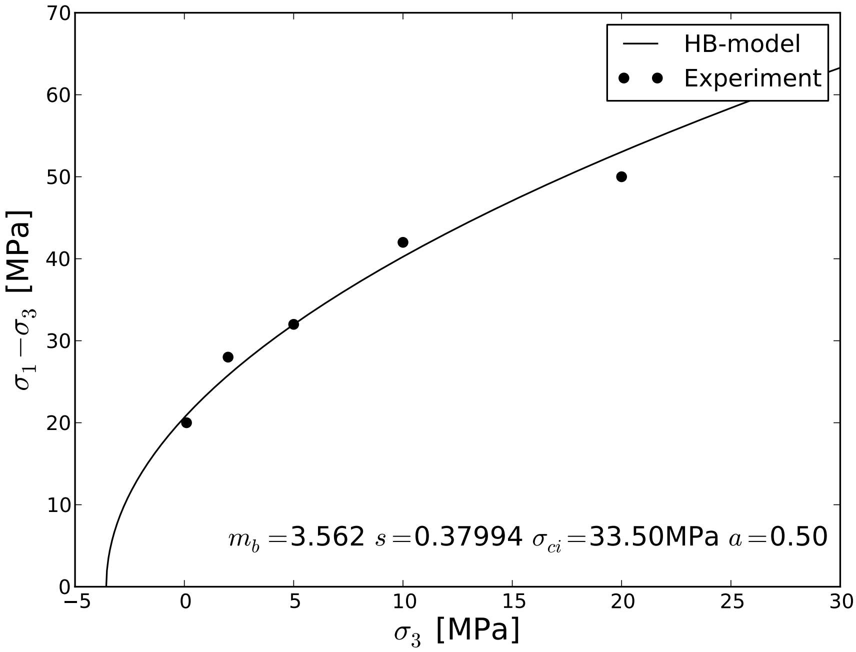

Best fit for experimental HB yield surface

In a similar manner (assuming $a_o^{res} = a = 0.5$) σ_{sf}, m_{bo}^{res} and s_o^{res} were optimized by minimizing error functional F_2

$$F_2(s_o^{res}, m_{bo}^{res}) = \sum_{i=1}^{N=5} \left(1 - \frac{q_f^{res-theor}(\sigma_{3i})}{q_{fi}^{res-exp}} \right)^2$$

$$q_f^{res-theor}(\sigma_{3i}) = \sigma_{ci} \left(m_b^{res} \frac{\sigma_3}{\sigma_{ci}} + s^{res} \right)^{a^{res}}$$

It has to be mentioned that m_b^{res} and s^{res}, appearing in the expression for $q_f^{res-theor}(\sigma_{3i})$ depend on σ_3 value (see Win.2-10)

Result of this optimization assuming that σ_{sf} is a free parameter is shown in figure below.

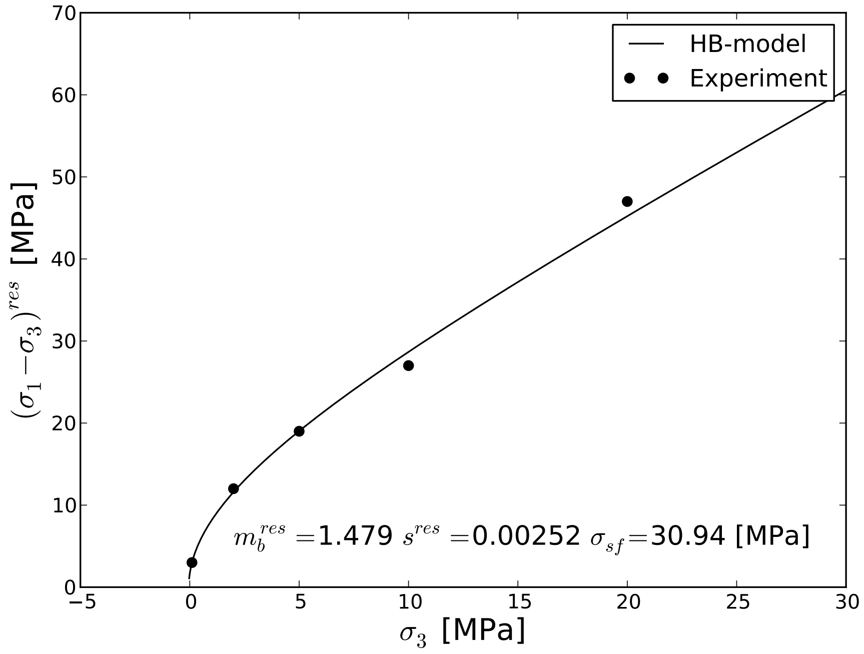

Residual values of ultimate shear stress in triaxial test (theory vs experiment) for σ_{sf} being a free parameter

Optimization of error functional F_2 with prescribed $\sigma_{sf} = f_c = \sigma_{ci}\ s^a$ yields result as in figure below. This check was made in order to indicate how to estimate σ_{sf} if it is missing. Comparing experimental and theoretical results one may say that the post-peak residual deviatoric stresses are reproduced in a very accurate manner in both cases.

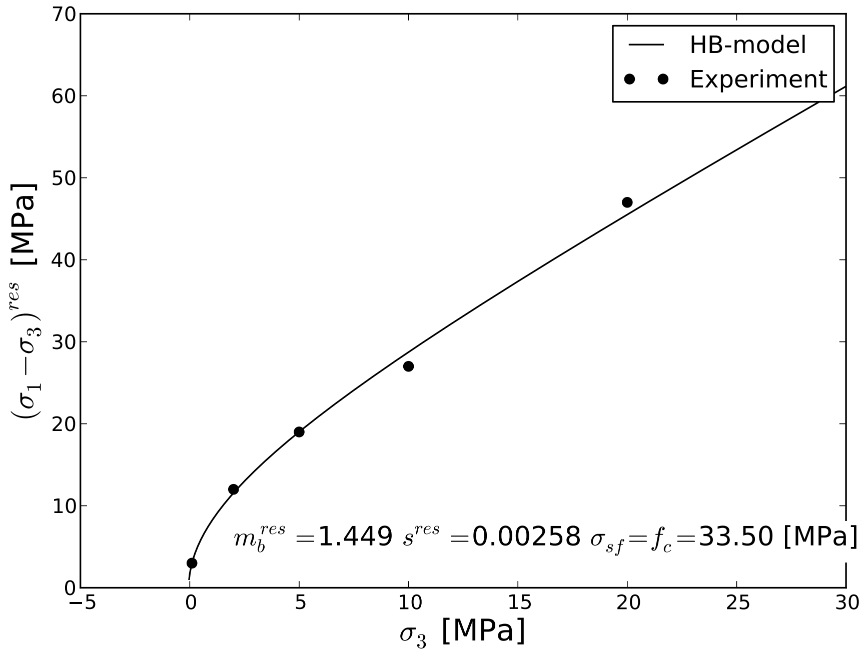

Residual values of ultimate shear stress in triaxial test (theory vs experiment) for prescribed σ_{sf} parameter

Set of parameters used in this test is given in the table below.

Group	Subgroup	Parameter	Unit	Value
Elastic		E	[MPa]	5600
		ν	[-]	0.3
Nonlinear	HB criterion	Definition		**Direct**
		GSI	[-]	unused
		D	[-]	unused
		m_i	[-]	unused
		σ_{ci}	[MPa]	33.5
		m_b	[-]	3.562
		s	[-]	0.38
		a	[-]	0.5
		☒ **Update E**		NO
	Rankine criterion	☒ **Rankine cut-off**	[-]	OFF
	Dilatancy	Type		◎ **Stress dep.**
		σ_ψ	[MPa]	33.5
		ψ	[deg]	30.0
		☒ **Strain dep.dil.**		ON
		f_ψ^o	[-]	0.0
		f_ψ^r	[-]	0.0
		f_ψ^{res}	[-]	1.0
	Hardening	☒ **Pre-peak hard.**		ON
		Type	[-]	*Standard*
		γ_r	[-]	0.008
		m_b^o	[-]	0.89
		s^o	[-]	0.095
		a^o	[-]	0.5
	Softening	☒ **Post-peak soft.**		ON
		γ_{res}	[-]	0.018
		m_{bo}^{res}	[-]	1.479
		s_o^{res}	[-]	0.003
		a_o^{res}	[-]	0.5
		σ_{sf}	[-]	30.94
		α^R	[-]	750 (not meaningful)
		☒ **Soft.regul.**		OFF
		Char.length	[m]	unused
		α	[-]	unused
		R	[m]	unused

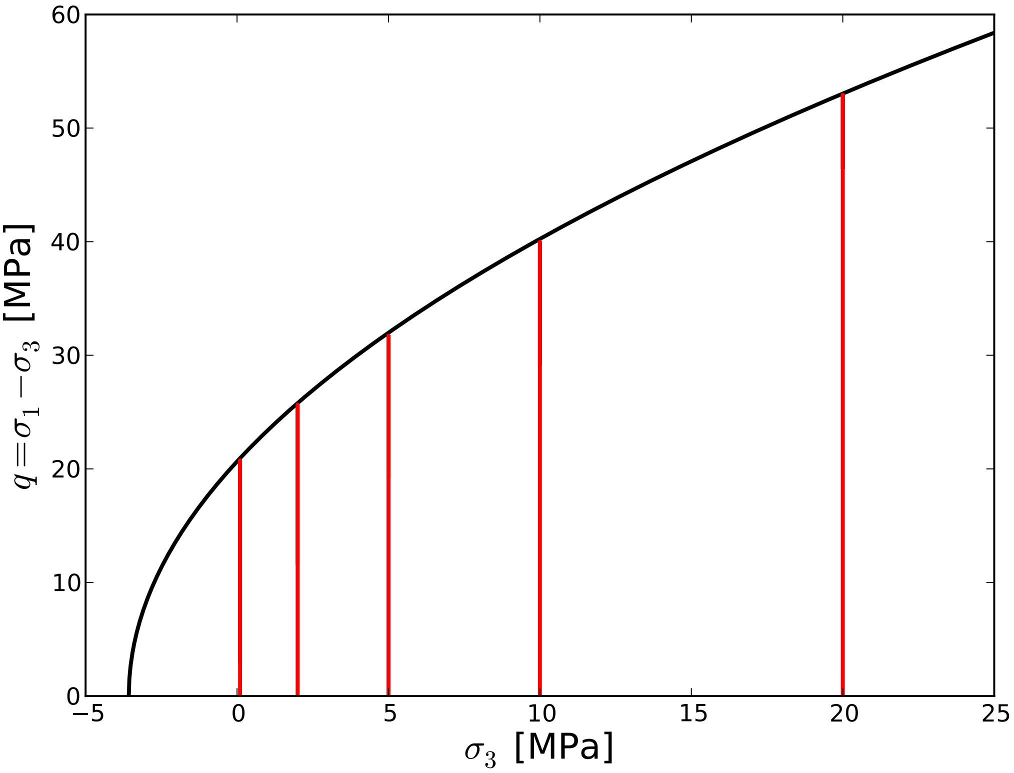

Stress paths in $q - \sigma_3$ axes

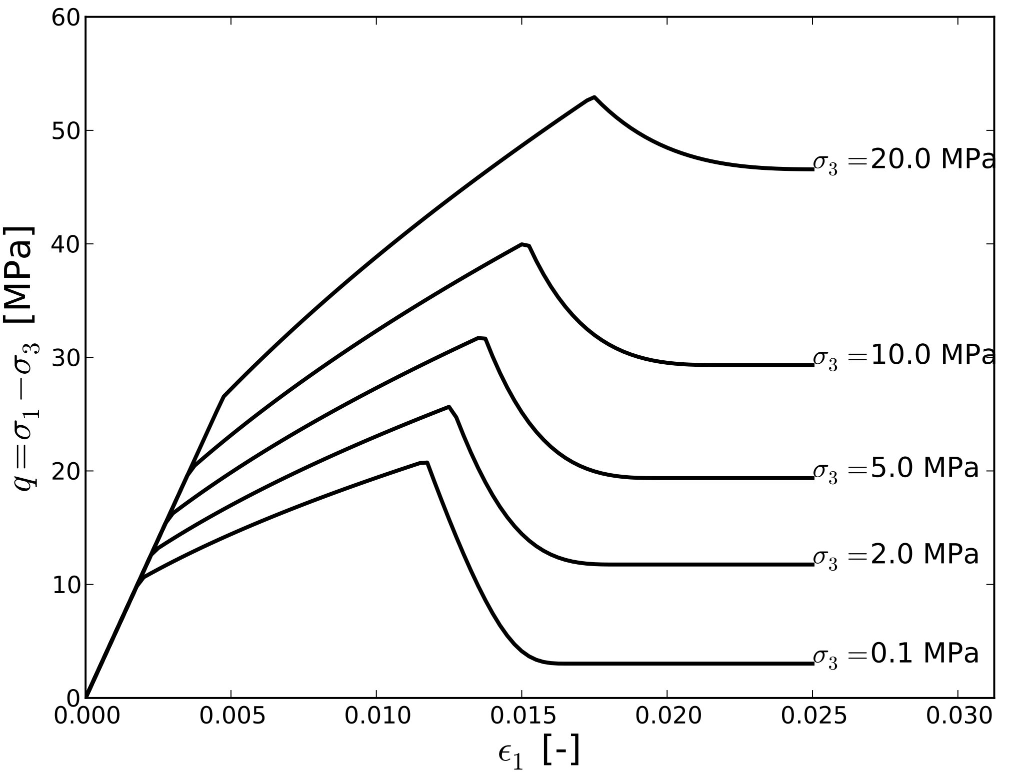

Shear characteristics $q = q(\varepsilon_1)$

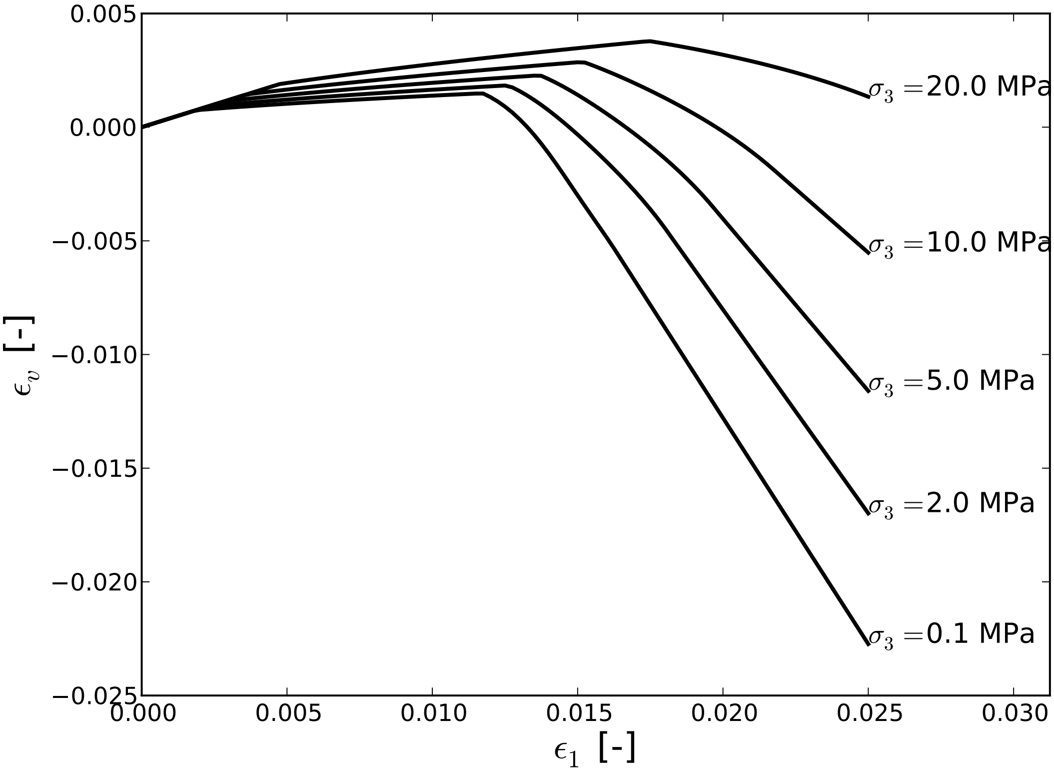

Dilatancy characteristics $\varepsilon_v = \varepsilon_1(\varepsilon_1)$

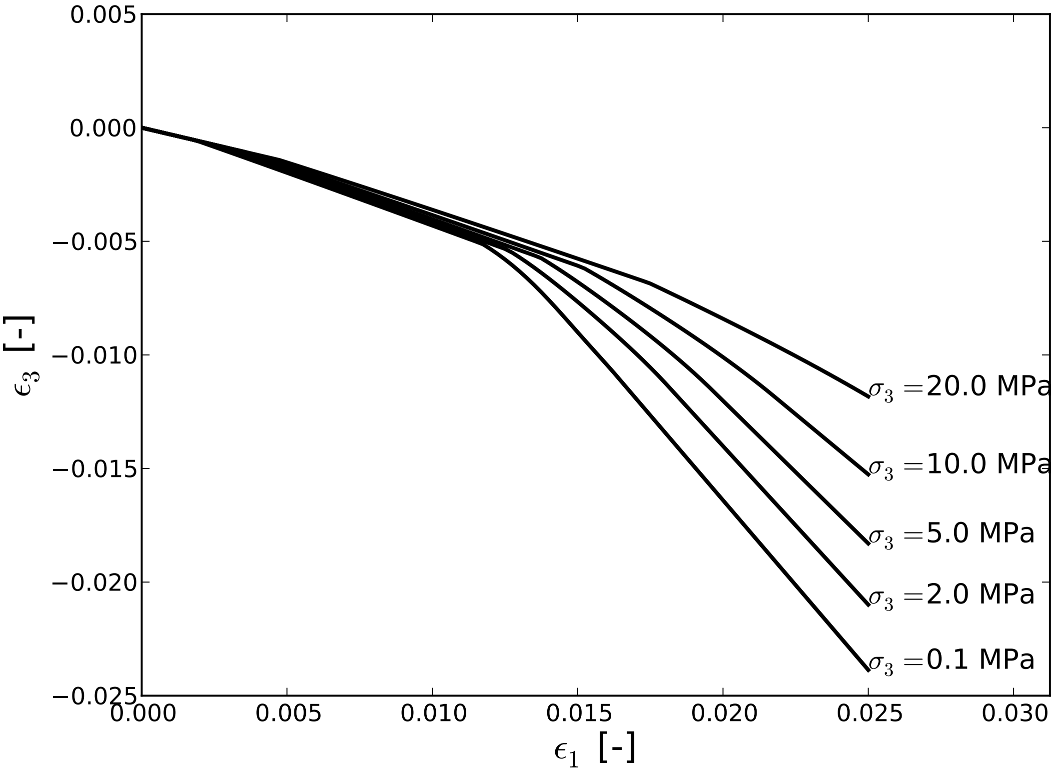

Dilatancy characteristics $\varepsilon_3 = \varepsilon_3(\varepsilon_1)$

4.4 Circular tunnel problem

Files: HB-circ-tunnel-axs-15m-INF.inp, HB-circ-tunnel-ps-15m-INF.inp

Problem of excavation of a circular tunnel in an elasto-plastic rock mass governed by H-B criterion and constant dilatancy angle ψ is analyzed in this section. (see Figure below). This problem can be solved in two formats i.e. axisymmetric and plane strain. Both cases are considered here. The initial stress state is defined by direct setting the effective stresses of value $\sigma_o = 20$ MPa with $K_o^{in\ situ} = 1$. The internal pressure p_i is assumed to be zero after the excavation.

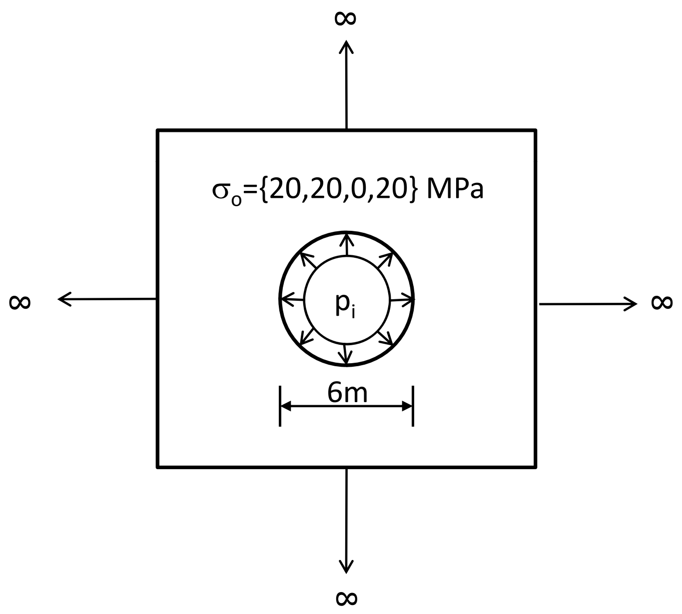

Geometry of the problem

To obtain highly accurate results with a very small mesh size one can make use of infinite elements. As infinite elements cannot be used in the initial state computation a standard model with surface load $q = 20$ kN/m^2 applied to both left and right vertical walls of the model is solved first (with assumed initial stresses σ_o), as shown in the Figure below. Later on a single element at the right wall of the mesh is excavated, while unbalance forces due to excavation are not dissipated (this can be made by applying a constant (with value 1.0) unloading function to that element), and axisymmetric elastic infinite element is added. This step does not produce any deformation. Once the infinite element is added we can perform an excavation of the tunnel that is simulated by decreasing the value of surface load, at the left vertical wall, up to the value $p_i = 0$. Assuming that a parameter in H-B model is equal to 0.5 one may solve this problem in an analytical manner (see [5]).

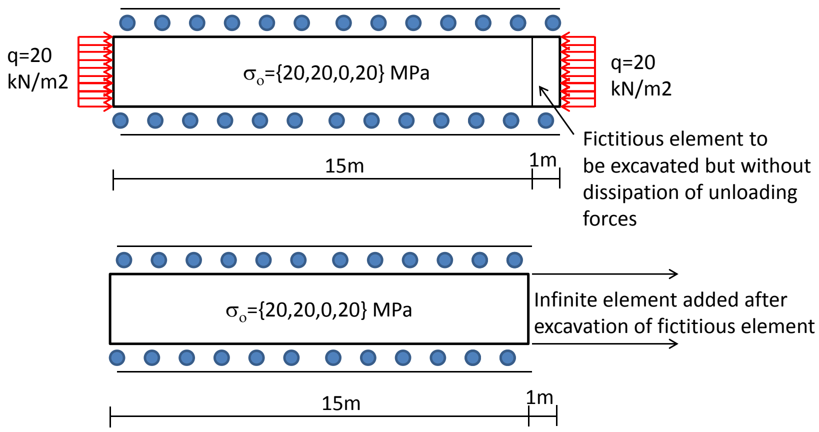

Geometry of the problem

Solution, in the elastic region ($r < R_p$), consists of the following set of expressions for radial and circumferential stresses, and radial displacement

$$
\begin{aligned}
\sigma_r &= \sigma_o - (\sigma_o - p_i^{cr}) \left(\frac{R_p}{r}\right)^2 \\
\sigma_\theta &= \sigma_o + (\sigma_o - p_i^{cr}) \left(\frac{R_p}{r}\right)^2 \\
u_r &= -\frac{1}{2G} (\sigma_o - p_i^{cr}) \frac{R_p^2}{r}
\end{aligned}
$$

The corresponding solution in the plastic region ($r < R_p$) takes the form

$$
\begin{aligned}
\sigma_r &= m_b\, \sigma_{ci} \left[\left(\sqrt{\frac{p_i^{cr}}{\sigma_{ci}\, m_b} + \frac{s}{m_b^2}} + \frac{1}{2} \ln\left(\frac{r}{R_p}\right) \right)^2 - \frac{s}{m_b^2} \right] \\
\sigma_\theta &= \sigma_r + \sigma_{ci} \sqrt{m_b \frac{\sigma_r}{\sigma_{ci}} + s}
\end{aligned}
$$

In the above expressions plastic radius R_p and the critical pressure p_i^{cr} are defined as

$$
\begin{aligned}
p_i^{cr} &= \frac{\sigma_{ci}\, m_b}{16} \left[1 - \sqrt{1 + 16 \left(\frac{\sigma_o}{\sigma_{ci}\, m_b} + \frac{s}{m_b^2} \right)} \right]^2 - \frac{s\, \sigma_{ci}}{m_b} \\
R_p &= R \exp \left[2 \left(\sqrt{\frac{p_i^{cr}}{\sigma_{ci}\, m_b} + \frac{s}{m_b^2}} - \sqrt{\frac{p_i}{\sigma_{ci}\, m_b} + \frac{s}{m_b^2}} \right) \right]
\end{aligned}
$$

$$u_r = \frac{1}{1-A_1}\left[\left(\frac{r}{R_p}\right)^{A_1} - A_1\frac{r}{R_p}\right] u_r(1) + \frac{1}{1-A_1}\left[\left(\frac{r}{R_p}\right) - \left(\frac{r}{R_p}\right)^{A_1}\right] u_r'(1) -$$
$$\frac{R_p}{2G}\left(\frac{\sigma_{ci} m_b}{4}\right)\frac{A_2-A_3}{1-A_1}\frac{r}{R_p}\left[\ln\left(\frac{r}{R_p}\right)\right]^2 -$$
$$\frac{R_p}{2G}\left(\sigma_{ci} m_b\right)\left[\frac{A_2-A_3}{(1-A_1)^2}\sqrt{\frac{p_i^{cr}}{\sigma_{ci} m_b} + \frac{s}{m_b^2}} - \frac{1}{2}\frac{A_2 - A_1 A_3}{(1-A_1)^3}\right] \times$$
$$\left[\left(\frac{r}{R_p}\right)^{A_1} - \frac{r}{R_p} + (1-A_1)\frac{r}{R_p}\ln\left(\frac{r}{R_p}\right)\right]$$

Coefficients $u_r(1)$, $u_r'(1)$, A_1, A_2, A_3 appearing in the expression for u_r are given as follows

$$\begin{aligned}
u_r(1) &= -\frac{R_p}{2G}\left(\sigma_o - p_i^{cr}\right)\\
u_r'(1) &= \frac{R_p}{2G}\left(\sigma_o - p_i^{cr}\right)\\
A_1 &= -K_\psi\\
A_2 &= 1 - \nu - \nu\, K_\psi\\
A_3 &= \nu - (1-\nu)\, K_\psi\\
K_\psi &= \frac{1+\sin\psi}{1-\sin\psi}
\end{aligned}$$

To run the benchmark same material data set, as in [5], is used (see table below).

Group	Subgroup	Parameter	Unit	Value
Elastic		E	[MPa]	2000
		ν	[-]	0.25
Nonlinear	HB criterion	Definition		**Direct**
		GSI	[-]	unused
		D	[-]	unused
		m_i	[-]	unused
		σ_{ci}	[MPa]	50.0
		m_b	[-]	1.6768
		s	[-]	3.8659^{-3}
		a	[-]	0.5
		☒ **Update E**		OFF
	Rankine criterion	☒ **Rankine cut-off**	[-]	OFF
	Dilatancy	Type		⊚ **Const.**
		σ_ψ	[MPa]	unused
		ψ	[deg]	10.0
		☒ **Strain dep.dil.**		OFF
	Hardening	☒ **Pre-peak hard.**		OFF

	Softening	☒ **Post-peak soft.**		OFF

As it is shown in the next two figures the theoretical results are very well reproduced by the FE model.

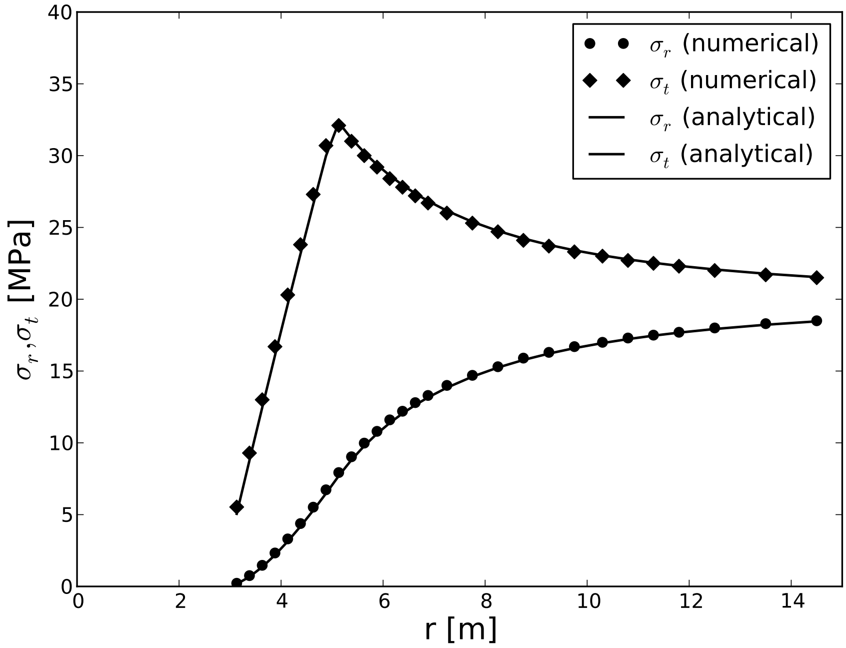

Distribution of radial and circumferential stresses

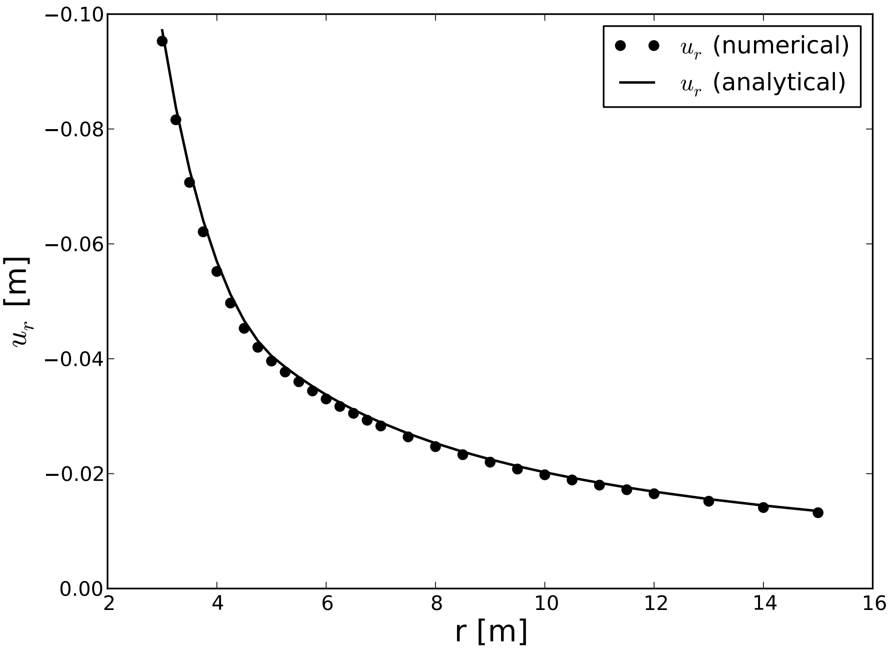

Distribution of radial displacements

4.5 Stability of a moderate slope

Files: Slope-35degs.inp

Stability of a moderate slope inclined at 35^o is analyzed in this section. The material data is taken from paper by Benz et al. [1] (m_b, s and a H-B model parameters are derived based on given GSI index and disturbance factor D).

Group	Subgroup	Parameter	Unit	Value
Elastic		E	[kPa]	410734
		ν	[-]	0.3
Nonlinear	HB criterion	Definition		**GSI**
		GSI	[-]	5
		D	[-]	0
		m_i	[-]	2
		σ_{ci}	[kPa]	30000
		☒ **Update E**		ON
	Rankine criterion	☒ **Rankine cut-off**	[-]	OFF
	Dilatancy	Type		◎ **Const.**
		σ_ψ	[MPa]	unused
		ψ	[deg]	10.0

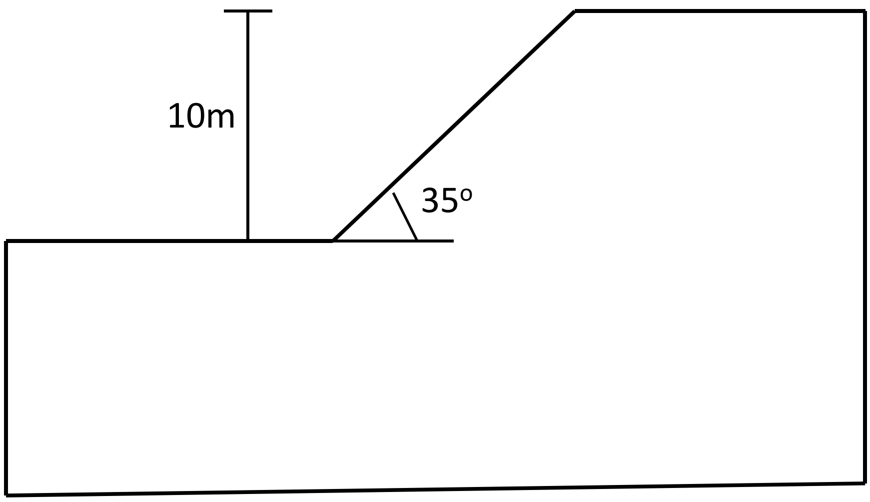

Geometry of the slope

The failure state, visualized in figure below, was achieved for safety factor 1.58. In the paper by Benz et al. the authors achieved SF =1.51, however it is not known what value of dilatancy angle was used in their analysis.

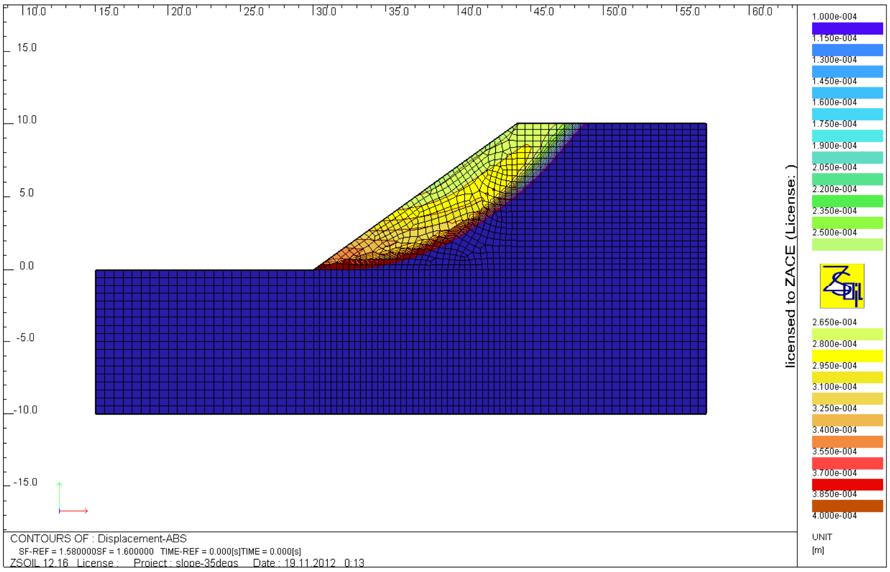

Failure pattern

4.6 Strain localization in biaxial compression

File: HB-biaxial-compression-mesh-x1c.inp, HB-biaxial-compression-mesh-x2c.inp

Analysis of strain localization problem in biaxial compression test is the aim of this example. A 0.2m x 0.4m block, shown in figure below, (with isotropic initial compressive stresses $\sigma_o =$ 0 MPa) is subjected to imposed vertical displacements. All nodes at the top and bottom are fixed in the horizontal direction. The softening scaling is used assuming characteristic length value to be L_c=0.03m. The two meshes are used 10 x 20 and 20 x 40 elements.

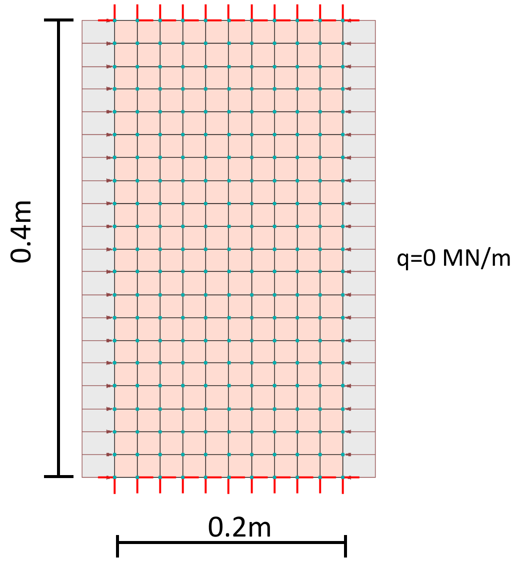

Geometry of the sample

Set of parameters used in this test is given in the table below.

Group	Subgroup	Parameter	Unit	Value
Elastic		E	[MPa]	10000
		ν	[-]	0.3
Nonlinear	HB criterion	Definition		**Direct**
		GSI	[-]	unused
		D	[-]	unused
		m_i	[-]	unused
		σ_{ci}	[MPa]	33.5
		m_b	[-]	2
		s	[-]	0.128
		a	[-]	0.5
		☒ **Update E**		NO
	Rankine criterion	☒ **Rankine cut-off**	[-]	ON
		$\|f_t\|$	[MPa]	1.0
	Dilatancy	Type		⊙ **Constant**
		σ_ψ	[MPa]	unused
		ψ	[deg]	16.84
		☒ **Strain dep.dil.**		ON
		f_ψ^o	[-]	0.0
		f_ψ^r	[-]	0.545131
		f_ψ^{res}	[-]	1.0
	Hardening	☒ **Pre-peak hard.**		ON
		Type	[-]	*Standard*
		γ_r	[-]	0.0058
		m_b^o	[-]	0.42985
		s^o	[-]	0.0821207
		a^o	[-]	0.5
	Softening	☒ **Post-peak soft.**		ON
		γ_{res}	[-]	0.0155
		m_{bo}^{res}	[-]	0.832175
		s_o^{res}	[-]	0.0001
		a_o^{res}	[-]	0.5
		σ_{sf}	[-]	22.6375
		α^R	[-]	750.0
		☒ **Soft.regul.**		ON (Softening scaling)
		Char.length	[m]	0.03
		α	[-]	unused

Strain localization pattern for coarser mesh and the corresponding force-displacement diagram are shown in the first figure below. Result for dense mesh (2x2 split on coarser one) is shown in the second figure. Force-displacement diagrams for both meshes show practical mesh independence of results.

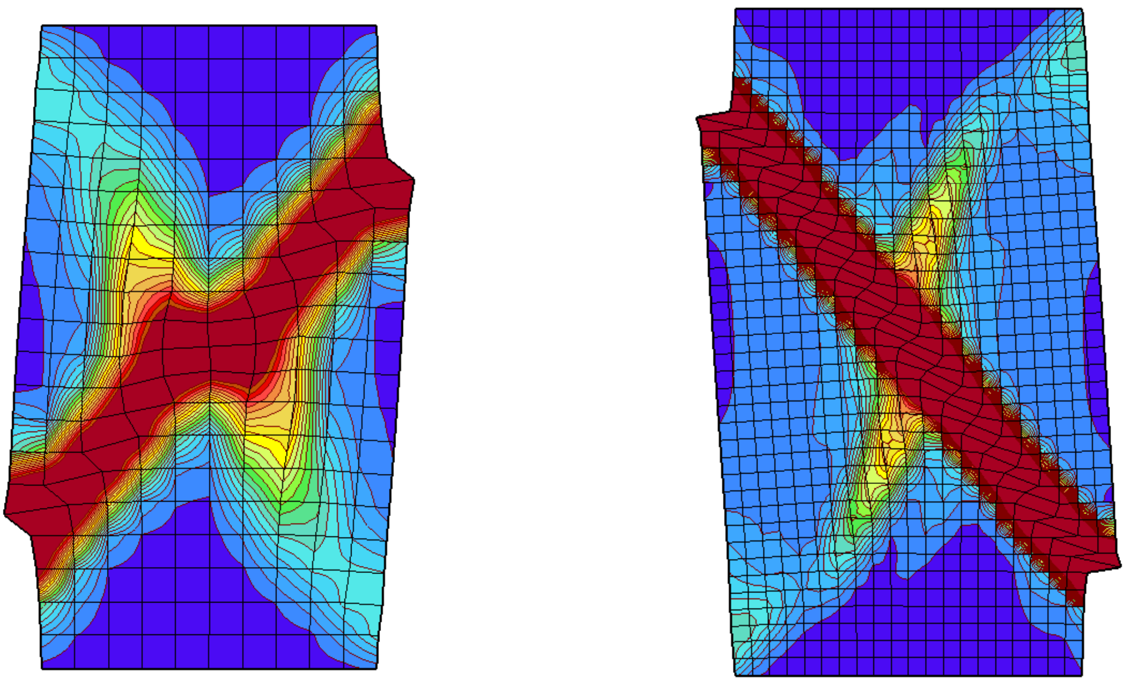

Strain localization pattern for two meshes

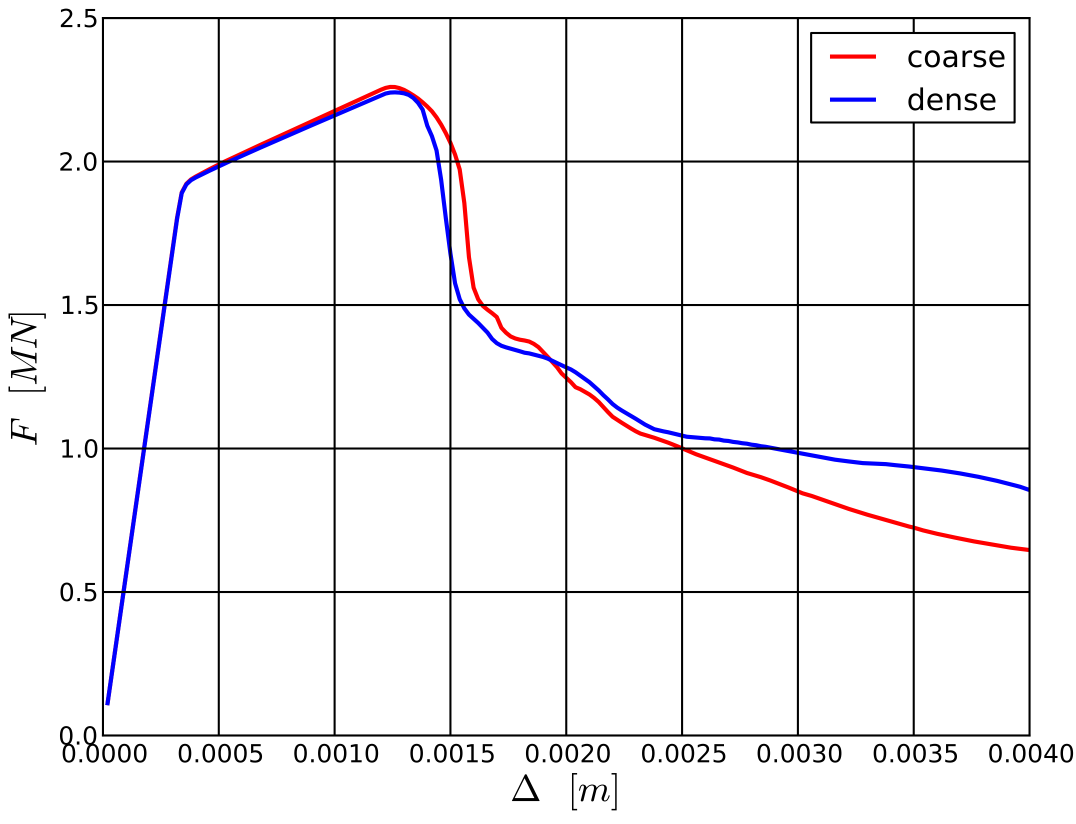

Comparizon of force-displacement diagrams for two meshes

4.7 Strain localization analysis for triaxial compression tests

Files:
triax-3D-mesh-1-0_1MPa-Lc-2cm,
triax-3D-mesh-1-2MPa-Lc-2cm,
triax-3D-mesh-1-5MPa-Lc-2cm,
triax-3D-mesh-1-10MPa-Lc-2cm,
triax-3D-mesh-1-0_1MPa-Lc-3mm

Analysis of 3D strain localization in the triaxial compression test is the matter of this section. The analyzed sample is 54mm wide and 108 mm high. All nodes at the bottom boundary are fully fixed while imposed vertical displacements are applied at the top boundary (5mm at the end of loading). Creep effects are neglected and no extra material, neither geometrical (except discretization) imperfections, are introduced. Four confining stresses, represented by equivalent external pressures, are analyzed i.e. $\sigma_3 = 0.1, 2.0, 5.0, 10.0$ MPa. The initial stress state corresponding to the assumed confining stress σ_3 is defined through the initial effective stress super-element in all four cases. Finite element mesh is shown in the figure 4.1. Deformed meshes for all four confining stresses, plot at end of the loading, are shown in fig.4.2, 4.3, 4.4 and 4.5. Evolution of sum of vertical nodal reactions diminished by sum of their values at the initial state is shown in fig.4.6. Influence of characteristic length L_c on force-displacement diagram, for case of σ_3 =0.1 MPa, is shown in fig.4.7.
It has to be emphasized here that for problems with softening, run under displacement control, special attention must be paid to the values of assumed convergence norm tolerances. For unbalance forces we should use $TOL_{RHS} < 10^{-4}$ and for the energy norm $TOL_E < 10^{-5}$ for most of the problems. For force controled problems the standard tolerance $TOL_{RHS} = 0.01$ can also be too high.

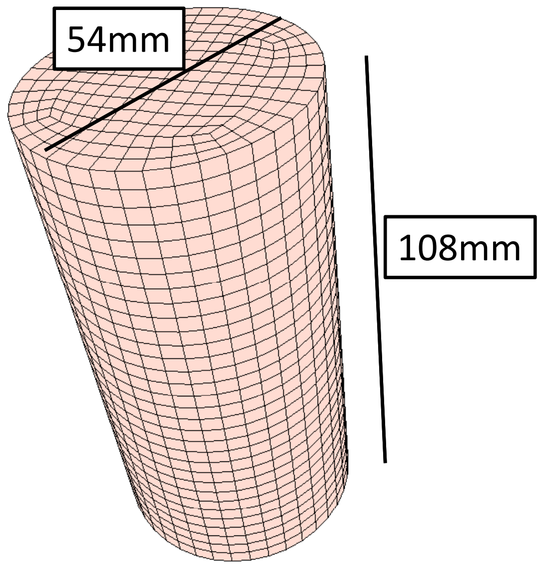

Figure 4.1: FE mesh

Material properties used in all simulations are given in the following table

Table 4.7: Material parameters

Group	Subgroup	Parameter	Unit	Value
Elastic		E	[MPa]	4000
		ν	[-]	0.3
Nonlinear	HB criterion	Definition		**Direct**
		GSI	[-]	unused
		D	[-]	unused
		m_i	[-]	unused
		σ_{ci}	[MPa]	33.5
		m_b	[-]	2
		s	[-]	0.128
		a	[-]	0.5
		☒ **Update E**		NO
	Rankine criterion	☒ **Rankine cut-off**	[-]	ON
		$\|f_t\|$	[MPa]	1.2
	Dilatancy	Type		◎ **Constant**
		σ_ψ	[MPa]	unused
		ψ	[deg]	16.84
		☒ **Strain dep.dil.**		ON
		f_ψ^o	[-]	0.0
		f_ψ^r	[-]	0.545131
		f_ψ^{res}	[-]	1.0
	Hardening	☒ **Pre-peak hard.**		ON
		Type	[-]	*Standard*
		γ_r	[-]	0.0058
		m_b^o	[-]	0.42985
		s^o	[-]	0.0821207
		a^o	[-]	0.5
	Softening	☒ **Post-peak soft.**		ON
		γ_{res}	[-]	0.0155
		m_{bo}^{res}	[-]	0.832175
		s_o^{res}	[-]	0.0080196
		a_o^{res}	[-]	0.5
		σ_{sf}	[-]	22.6375
		α^R	[-]	750.0
		☒ **Soft.regul.**		Soft.scaling
		Char.length	[m]	0.02
		α	[-]	unused
	Creep	☒ **Viscopl.creep**		OFF

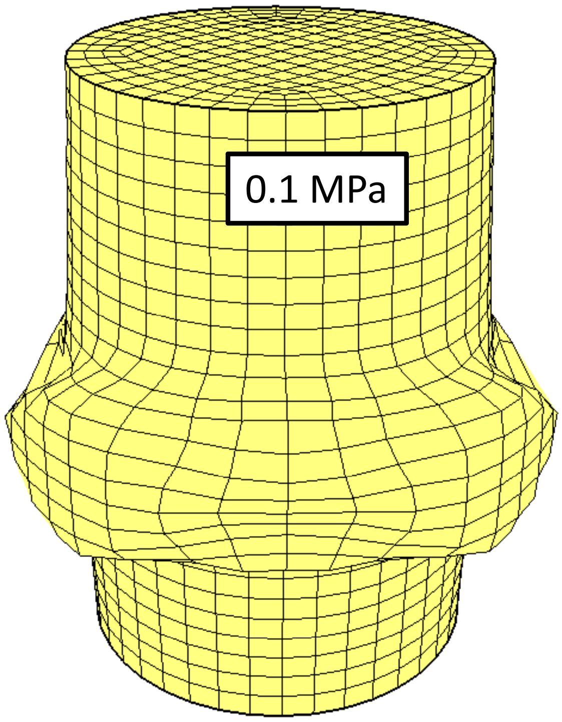

Figure 4.2: Deformed mesh at end of loading ($\Delta_y = 5$ mm) for $\sigma_3 = 0.1$ MPa

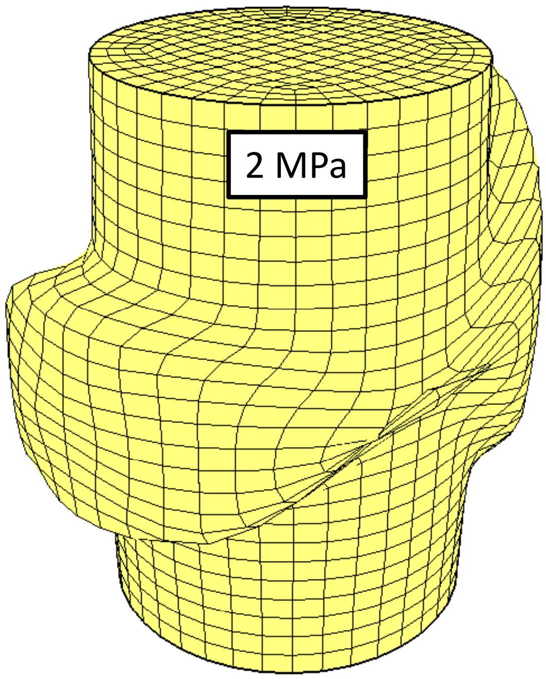

Figure 4.3: Deformed mesh at end of loading ($\Delta_y = 5$ mm) for $\sigma_3 = 2$ MPa

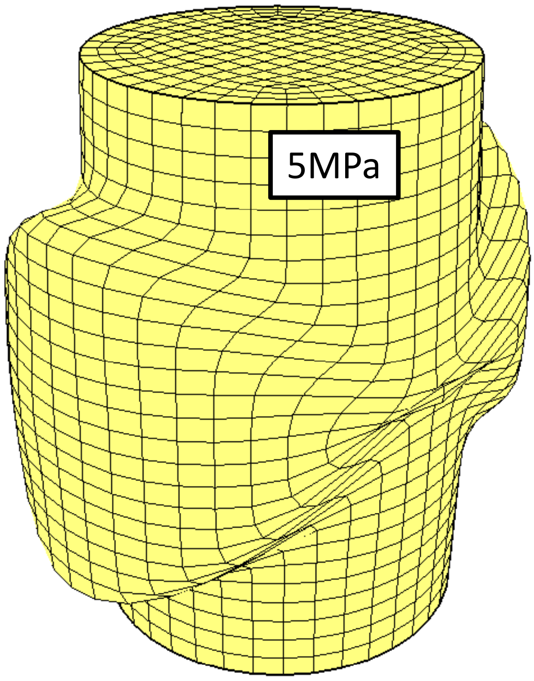

Figure 4.4: Deformed mesh at end of loading ($\Delta_y = 5$ mm) for $\sigma_3 = 5$ MPa

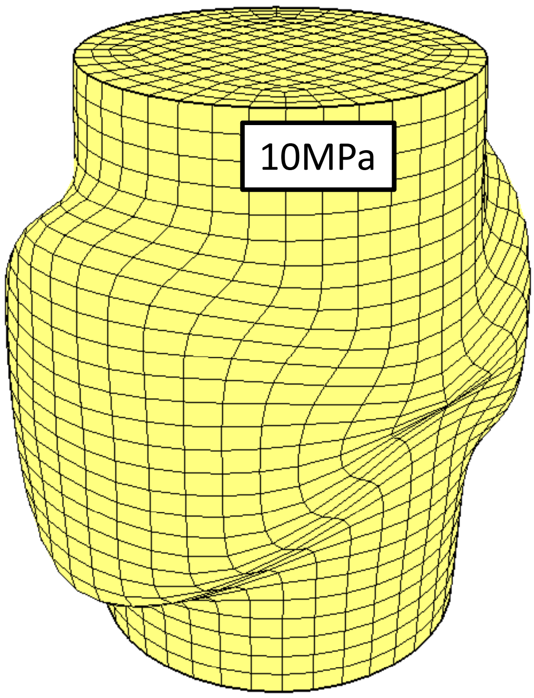

Figure 4.5: Deformed mesh at end of loading ($\Delta_y = 5$ mm) for $\sigma_3 = 10$ MPa

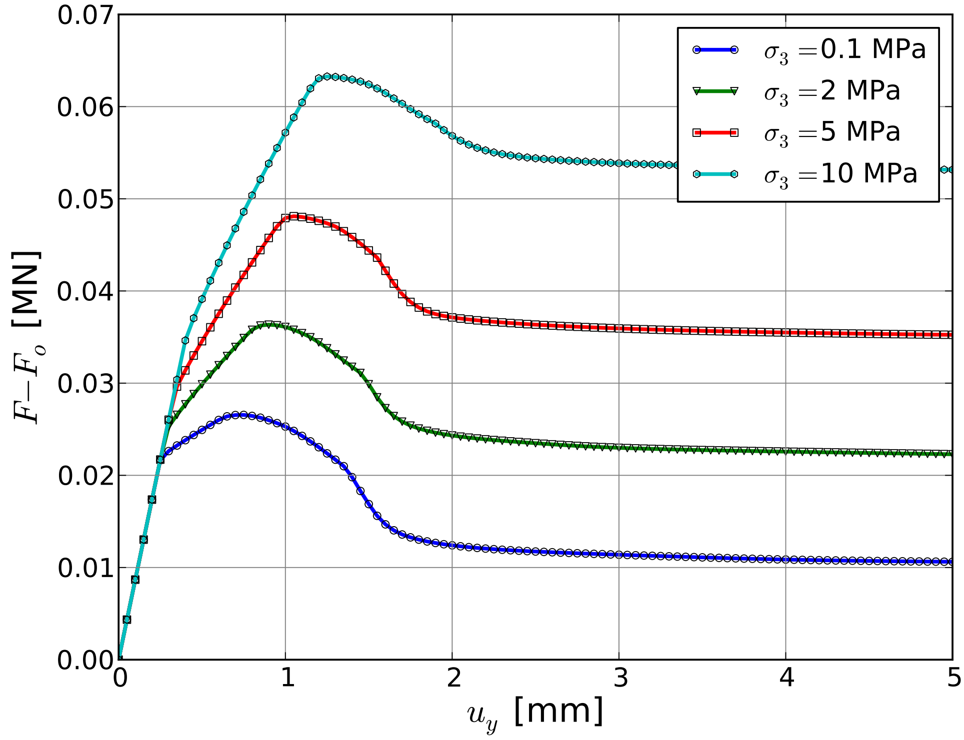

Figure 4.6: Force-displacement diagrams for different σ_3 values and $L_c = 20$ mm

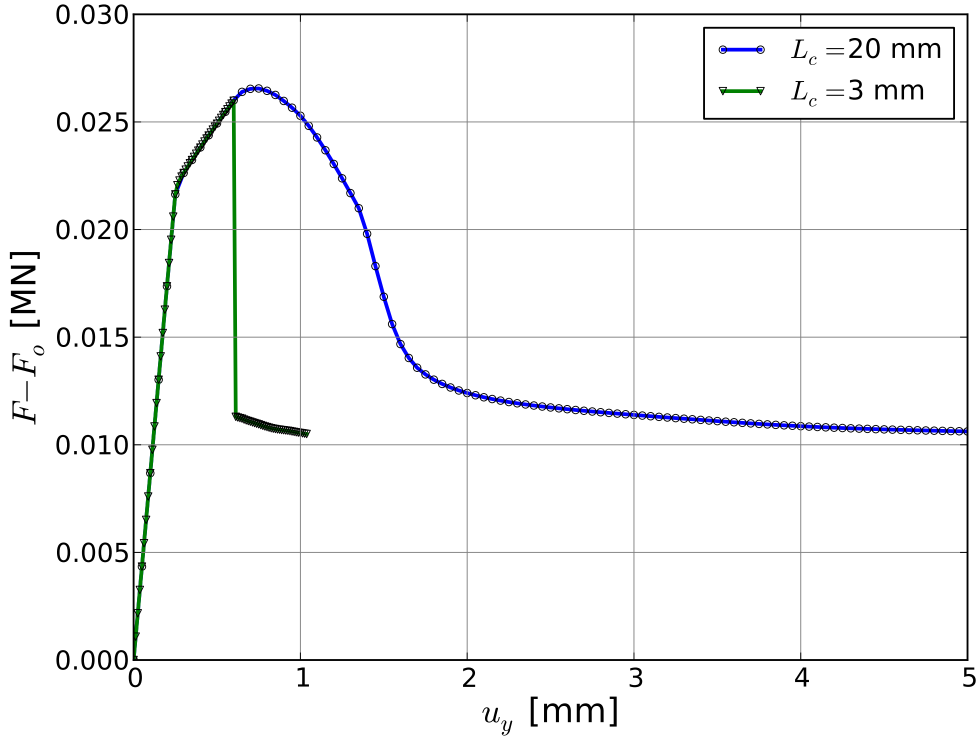

Figure 4.7: Force-displacement diagrams for different L_c values at σ_3 = 0.1 MPa

Bibliography

[1] T. Benz, R. Schwab, R. Kauther, and P. Vermeer. A Hoek-Brown criterion with intrinsic material strength factorization. *International Journal of Rock Mechanics and Mining Sciences*, 45:210–222, 2008.

[2] E. Hoek, C. C. Torres, and B. Corkum. Hoek-Brown failure criterion - 2002 edition. In *Proceedings of the North American Rock Mechanics Symposium*, Toronto, 2002.

[3] S. Pietruszczak and Z. Mróz. Finite element analysis of deformation of strain-softening materials. *International Journal for Numerical Methods in Engineering*, 17:327–334, 1981.

[4] M. Souley, G. Armand, K. Su, and M. Ghoreychi. Modeling the viscoplastic and damage behavior in deep argillaceous rocks. *Physics and Chemistry of the Earth*, 36, 2011.

[5] C. C. Torres. Elasto-plastic solution of tunnel problem using the generalized form of Hoek-Brown failure criterion. *International Journal of Rock Mechanics and Mining Sciences*, 41:629–639, 2004.

[6] A. Truty, Th. Zimmermann, K. Podleś, R. Obrzud with contribution by A. Urbański and S. Commend and Jean-Luc Sarf Z_Soil manual. *Elmepress and Zace Services Limited*, ,2013.